International Journal of
Molecular Sciences

MDPI

Article

Solvatochromic Sensitivity of BODIPY Probes: A New Tool for Selecting Fluorophores and Polarity Mapping

Felix Y. Telegin [1], Viktoria S. Karpova [2], Anna O. Makshanova [3], Roman G. Astrakhantsev [4] and Yuriy S. Marfin [1,*]

[1] G.A. Krestov Institute of Solution Chemistry of the RAS, 153045 Ivanovo, Russia
[2] Department of Inorganic Chemistry, Ivanovo State University of Chemistry and Technology, 153000 Ivanovo, Russia
[3] Department of Natural Sciences, Mendeleev University of Chemical Technology of Russia, 125047 Moscow, Russia
[4] HSE Tikhonov Moscow Institute of Electronics and Mathematics, HSE University, 101000 Moscow, Russia
* Correspondence: ymarfin@gmail.com

Abstract: This research work is devoted to collecting a high-quality dataset of BODIPYs in a series of 10–30 solvents. In total, 115 individual compounds in 71 solvents are represented by 1698 arrays of the spectral and photophysical properties of the fluorophore. Each dye for a series of solvents is characterized by a calculated value of solvatochromic sensitivity according to a semiempirical approach applied to a series of solvents. The whole dataset is classified into 6 and 24 clusters of solvatochromic sensitivity, from high negative to high positive solvatochromism. The results of the analysis are visualized by the polarity mapping plots depicting, in terms of wavenumbers, the absorption versus emission, stokes shift versus − (absorption maxima + emission maxima), and quantum yield versus stokes shift. An analysis of the clusters combining several dyes in an individual series of solvents shows that dyes of a high solvatochromic sensitivity demonstrate regular behaviour of the corresponding plots suitable for polarity and viscosity mapping. The fluorophores collected in this study represent a high quality dataset of pattern dyes for analytical and bioanalytical applications. The developed tools could be applied for the analysis of the applicability domain of the fluorescent sensors.

Keywords: BODIPY; fluorescent probe; absorption; emission; solvatochromic sensitivity; biosensing

Citation: Telegin, F.Y.; Karpova, V.S.; Makshanova, A.O.; Astrakhantsev, R.G.; Marfin, Y.S. Solvatochromic Sensitivity of BODIPY Probes: A New Tool for Selecting Fluorophores and Polarity Mapping. *Int. J. Mol. Sci.* **2023**, *24*, 1217. https://doi.org/10.3390/ijms24021217

Academic Editors: Grigory Zyryanov and Sougata Santra

Received: 31 October 2022
Revised: 21 December 2022
Accepted: 28 December 2022
Published: 7 January 2023

1. Introduction

Currently, the solvatochromic properties of BODIPY sensors and other efficient probes are being extensively explored in analytical [1,2], bio, and medicinal chemistry [3–7] due to their high sensitivity and their selectivity to environmental macro- and micro-polarity. A wide variety of BODIPYs and other fluorophores are reported in scientific papers and a design strategy for future applications is developed [8–12]. Numerous examples have recently been reviewed for polarity sensitive probes of various subcellular structures [13–16], reactive oxygen and nitrogen species [17,18], viscosity sensitive probes based on the rotor effect [19–21] and AIE-effect [22–24], polarity-controlled triplet photosensitizers for photodynamic therapy [25–27], photoswitches, and photocages for theranostic applications [28–32], among others. In some cases, the insensitivity of BODIPY sensors to solvent polarity makes them ideal for bioimaging [15,33,34].

Routine information regarding the spectral and photophysical properties of dyes important for the further development of BODIPY fluorophores and discussions regarding their structure–property relationships are dispersed in numerous papers and reviews that have been published within the last two decades. In the original research, several libraries of BODIPY for intracellular cell imaging have been reported for individual solvents, namely: dimethylsulfoxide [35–40], methanol [41,42], and HEPES buffer solution [43].

Much of the information summarizing and arranging the properties of the fluorophores of diverse structures, including BODIPY dyes, in various solvents is provided in the extensive experimental databases, regarding the optical and photophysical properties needed for analyses [44–48].

One of the key strategies for the design and optimization of fluorescent sensors is focused on the polarity mapping of biological tissue. Several structures based on BODIPY scaffolds exemplify selected polarity probes developed in numerous research works [8,49–54]. Other prevalent scaffolds such as coumarin, xanthene, cyanine, pyrene, naphthalene, carbazole, porphyrin, phthalocyanine, and some others are also intensively discussed [15,55].

The above libraries present useful data for analysis and for seeking target molecules satisfying the requirements of the spectral and photophysical properties, sensitivity to surrounding media, selectivity for adsorption on biological tissue, etc. An examination of the above libraries shows a lack of data for selecting BODIPY fluorophores, which could serve as analytical templates for polarity.

Recent progress in the quantification of the solvatochromism of BODIPY probes [56,57] is promising for the further development of polarity-based approaches for tailoring the structure of fluorophores. Data of such kind have not been systematically analyzed in the literature. Therefore, the current research aims at collecting high quality, low scale datasets for the analysis of the spectral absorption and emissions of BODIPY fluorophores, as well as the quantum yield in a long series of solvents (above 10) within a wide range of polarities, and a corresponding analysis of the effects in terms of the relationship of the spectral properties and the solvatochromic sensitivity of the compounds.

2. Results

2.1. Overview of the Properties of Solvatochromic BODIPYs and Solvents Explored in the Dataset

The list of fluorescent dyes selected for the research is shown in Table 1.

Table 1. List of dyes selected for the dataset.

1998 Lopez–Arbeloa–PM567 [58]
1999 Lopez–Arbeloa(177)–PM546 [59]
2004 Banuelos Prieto(29)–PAr1Ac [60]
2004 Banuelos–Prieto(5503)–PM597 [61]
2004 Lopez–Arbeloa–PM650 [50]
2004 Shen–3d [62]
2004 Shen–4a [62]
2004 Shen–4b [62]
2004 Shen–4c [62]
2004 Shen–4e [62]
2004 Shen–4f [62]
2006 Baruah–1 [63]
2006 Qin(190)–1 [64]
2008 Qin–1 [51]
2009 Cieslik–Boczula–2CN [65]
2009 Cieslik–Boczula–4CN [65]
2009 Qin(11731)–1 [66]
2010 Chaudhuri–1b [67]
2010 Filarowski–1 [54]
2010 Filarowski–2 [54]
2010 Filarowski–3 [54]
2010 Leen(2016)–1 [68]
2010 Leen(2016)–2 [68]
2010 Leen(2016)–3 [68]
2011 Banuelos(3437)–BTAA [69]
2012 Boens(9621)–1 [70]
2012 Boens(9621)–2 [70]
2012 Boens(9621)–3 [70]

Table 1. *Cont.*

2012 Boens(9621)–4 [70]
2012 Boens(9621)–5 [70]
2012 Boens(9621)–6 [70]
2012 Yin–1 [71]
2012 Zhao–OH [72]
2013 Er–BDC–9 [37]
2013 Nano–TX(6) [73]
2013 Yang–TPA–BDP1 [74]
2013 Yang–TPA–BDP2 [74]
2013 Yang–TPA–BDP3 [74]
2014 Boens–10 [75]
2014 Boens–6 [75]
2014 Boens–8 [75]
2015 Caltagirone–Py–BODIPY [76]
2015 Feng–1 [77]
2015 Filarowski–A [78]
2015 Jiao–3 [79]
2015 Jiao–4 [79]
2015 Jiao–5 [79]
2015 Jiao–1 [79]
2015 Jiao–2 [79]
2015 Thorat–Dye 2 [80]
2015 Thorat–Dye 3 [80]
2015 Thorat–Dye 4 [80]
2015 Waddell–1 [81]
2015 Waddell–2 [81]
2015 Waddell–3 [81]
2015 Waddell–4 [81]
2015 Waddell–5 [81]
2015 Waddell–6 [81]
2016 Bacalum–1 [82]
2016 Gupta–1 [83]
2016 Marfin(1975)–2 [84]
2016 Marfin(1975)–3 [84]
2016 Marfin(1975)–4 [84]
2016 Marfin(1975)–5 [84]
2016 Orte–2–Ethyn [53]
2016 Orte–2–Ph [53]
2016 Orte–3–Ethyn [53]
2016 Orte–3–Ph [53]
2016 Orte–3–Styryl [53]
2016 Orte–8–Ethyn [53]
2016 Orte–8–Ph [53]
2016 Qin–1 [52]
2016 Telore–7 [85]
2016 Telore–7a [85]
2016 Vu–2 [86]
2016 Vu–3 [86]
2016 Zhu(35627)–BP–2 [87]
2017 Petrushenko(488)–1 [88]
2017 Sadak–15 [89]
2017 Suhina–1 [90]
2017 Thorat–Dye 1 [91]
2017 Thorat–Dye 2 [91]
2017 Zhang(2447)–Ph–TMBDP [92]
2018 Leen–BODIPY [93]
2018 Mallah–Bn–OH–BDY [94]
2018 Ordonez–Hernandez–mVP1 [95]
2018 Ordonez–Hernandez–mVP2 [95]
2018 Ordonez–Hernandez–mVP3 [95]

Table 1. *Cont.*

2018 Ripoll–2 [96]
2018 Ripoll–4 [96]
2018 Ripoll–6 [96]
2019 Ali–10 [97]
2019 Ali–12 [97]
2019 Ali–14 [97]
2019 Ali–16 [97]
2019 Ali–19 [97]
2019 Ali–2 [97]
2019 Ali–20 [97]
2019 Ali–21 [97]
2019 Ali–23 [97]
2019 Ali–6 [97]
2019 Ali–9 [97]
2019 Antina–2,2–CH2–bis(BODIPY) [98]
2019 Antina–2,3–CH2–bis(BODIPY) [98]
2019 Antina–3,3–CH2–bis(BODIPY) [98]
2019 Bai–NJ1060 [99]
2019 Guseva–BODIPY 1 [100]
2019 Kawakami–BFBODIPY–DMP–DMAS [101]
2019 Sevinc–TPy–BDP [102]
2019 Zhang(148)–BDP [103]
2020 Gonzalez–Vera–2 [104]
2020 Gonzalez–Vera–3 [104]
2020 Shen–BODIPY–DT [105]
2021 Vysnauskas–BODIPY2 [106]
2021 Vysnauskas–BODIPY3 [106]

A general overview of the spectral properties, Stokes shift, and quantum yield for the whole dataset is demonstrated by the frequency diagrams in Figure 1. The properties correspond to the whole range of 71 solvents depicted in Table S3 (Supplementary Information).

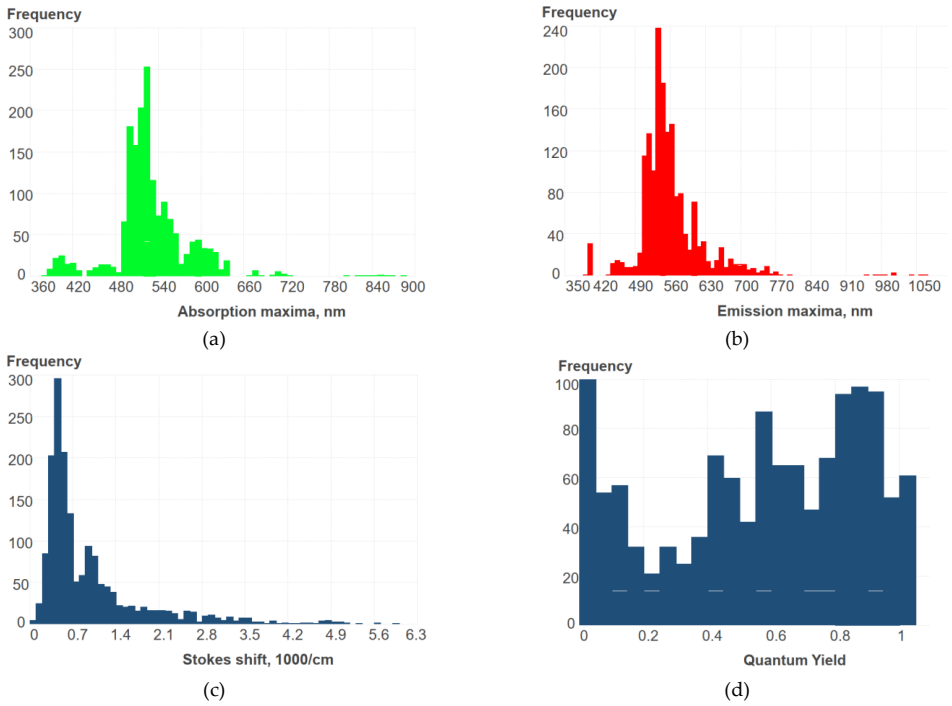

Figure 1. Frequency diagrams for a dataset of 115 BODIPYs: (**a**) absorption maxima; (**b**) emission maxima; (**c**) Stokes shift; (**d**) fluorescence quantum yield.

2.2. Cluster Analysis of the Solvatochromic Sensitivity

2.2.1. Six-Cluster Dataset of High Solvatochromic Sensitivity

The total dataset of 115 BODIPY dyes and 1698 combinations of dye and a solvent was divided into six clusters according to the solvatochromic sensitivity parameter A. The solvatochromic sensitivity (or polarity) of each compound in the whole dataset of BODIPY sensors varied in the range of −1.3 to +1.2. Each cluster combined several series of dyes, and a series of solvents for each dye appeared only once, according to the arrangements of the data.

Parameter A, representing solvatochromic sensitivity, was defined according to a method described in Section 3.3, through the use of the absorption and emission maxima of the fluorophore in a series of solvents.

The chemical structures of the BODIPY sensors classified according to the above procedure of clustering are provided in the six chats below (Schemes 1–6).

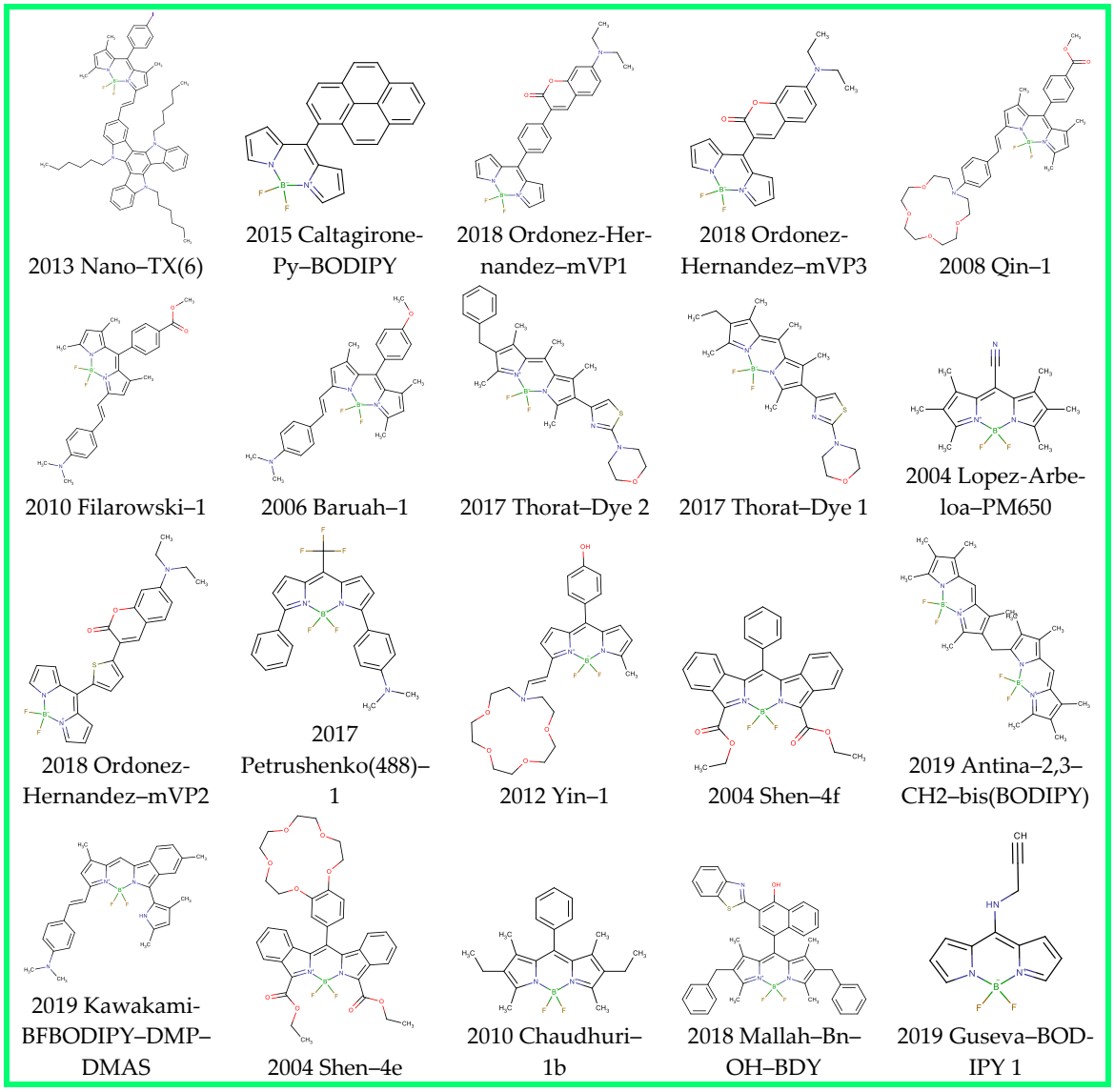

Scheme 1. Cluster 1; A: 1.18–0.24.

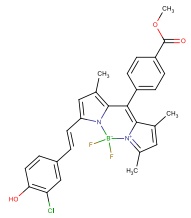

2006 Qin(190)–1

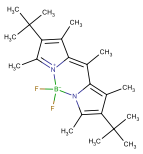

2015 Waddell–5

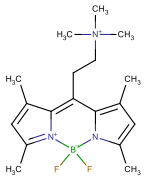

2016 Zhu(35627)–BP–2

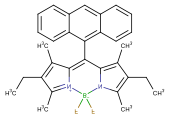

2016 Marfin(1975)–3

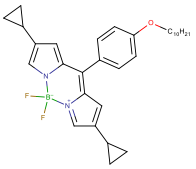

2021 Vysnauskas–BODIPY2

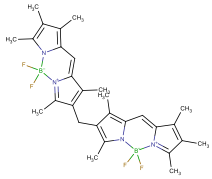

2019 Antina–3,3–CH2–bis(BODIPY)

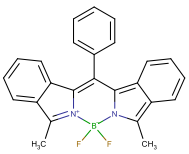

2004 Shen–4a

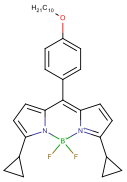

2021 Vysnauskas–BODIPY3

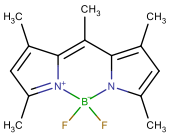

2015 Waddell–1

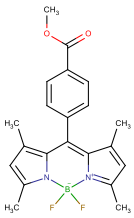

2017 Suhina–1

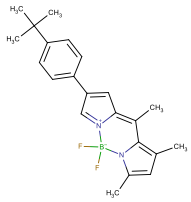

2016 Orte–2–Ph

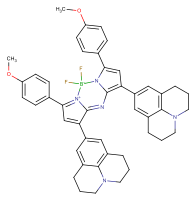

2019 Bai–NJ1060

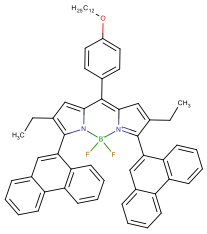

2016 Vu–2

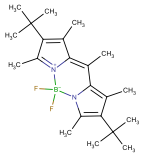

2004 Banuelos–Prieto(5503)–PM597

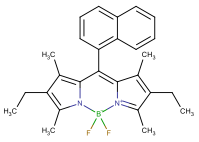

2016 Marfin(1975)–2

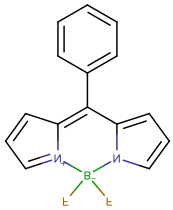

2016 Orte–8–Ph

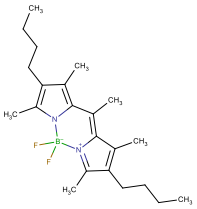

2015 Waddell–4

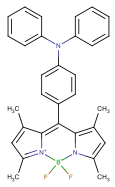

2013 Yang–TPA–BDP1

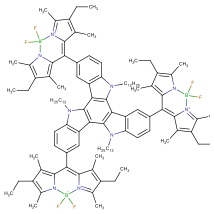

2017 Sadak–15

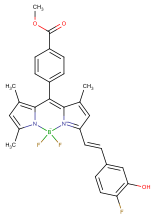

2010 Filarowski–3

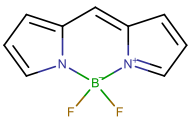

2019 Zhang(148)–BDP

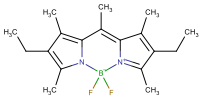

2015 Waddell–2

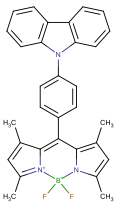

2016 Telore–7a

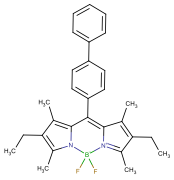

2016 Marfin(1975)–5

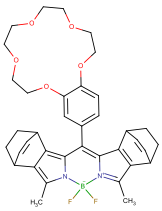

2004 Shen–3d

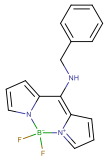

2014 Boens–8; 2018 Ripoll–2

Scheme 2. Cluster 2; A: 0.19–0.01.

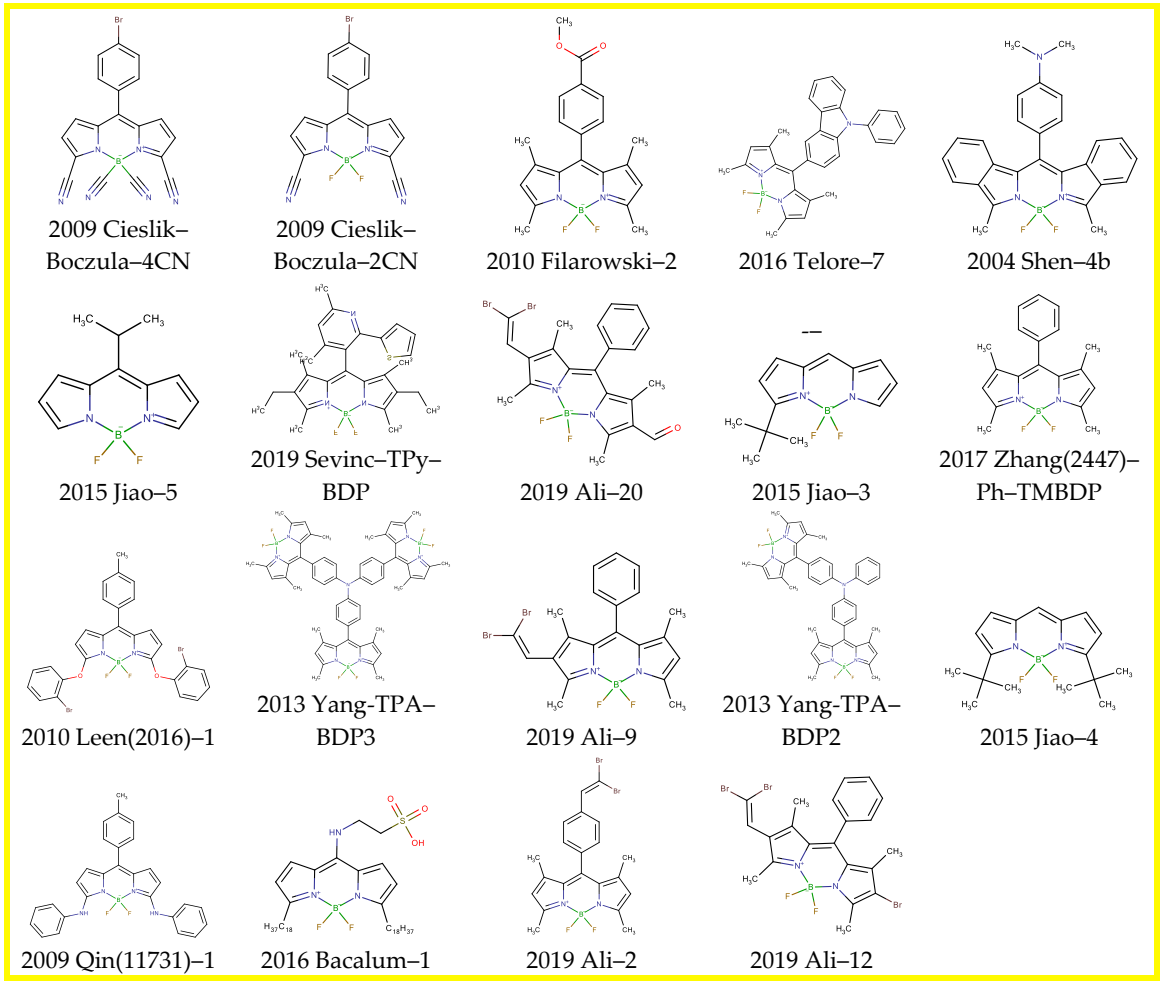

Scheme 3. Cluster 3; A: 0.01–(−0.04).

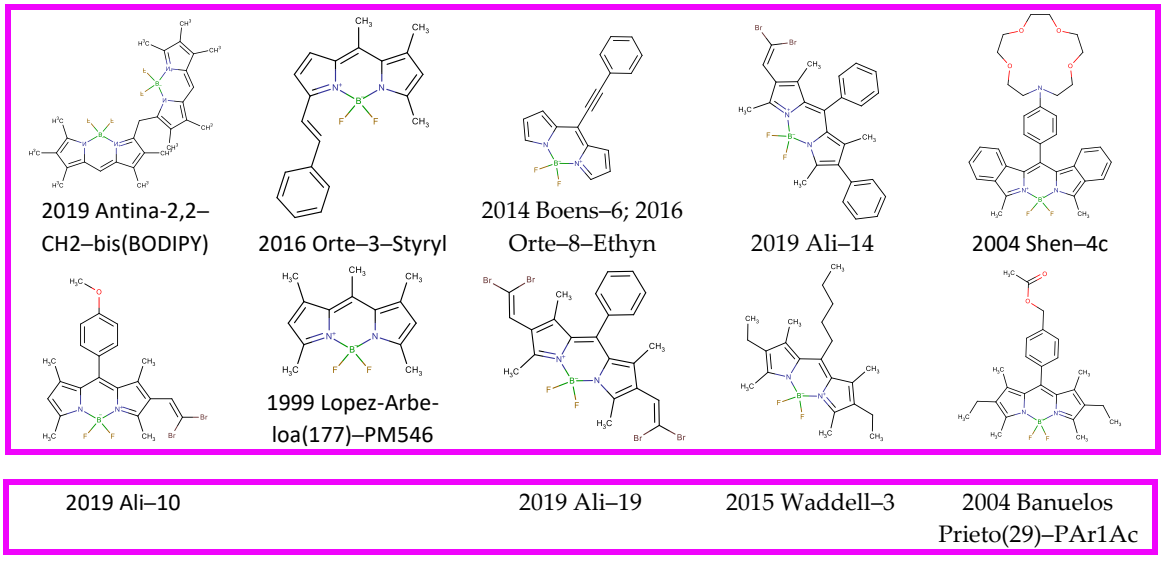

Scheme 4. Cluster 4; A: (−0.04)–(−0.11).

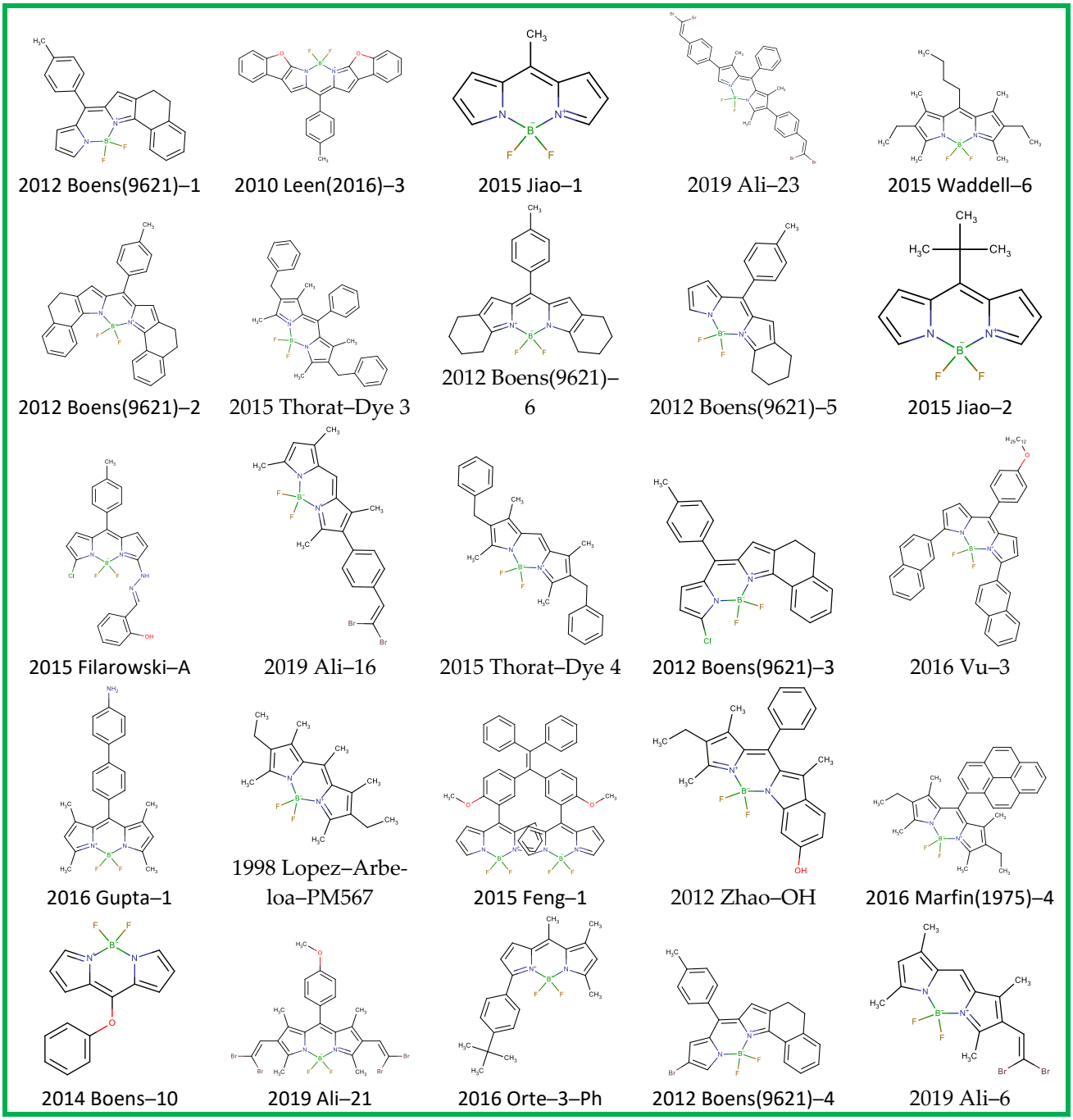

Scheme 5. Cluster 5; A: (−0.11)–(−0.25).

The spectral and photophysical properties of the dyes in the clusters are presented below in several diagrams. Figure 2 shows the relationship of the absorption maxima versus the emission maxima according to Equation (4) in terms of nm. Figure 3 demonstrates the relationship of the Stokes shift versus − (Absorption maxima + Emission maxima), which corresponds to the basic Equation (1) and is expressed in 1000/cm.

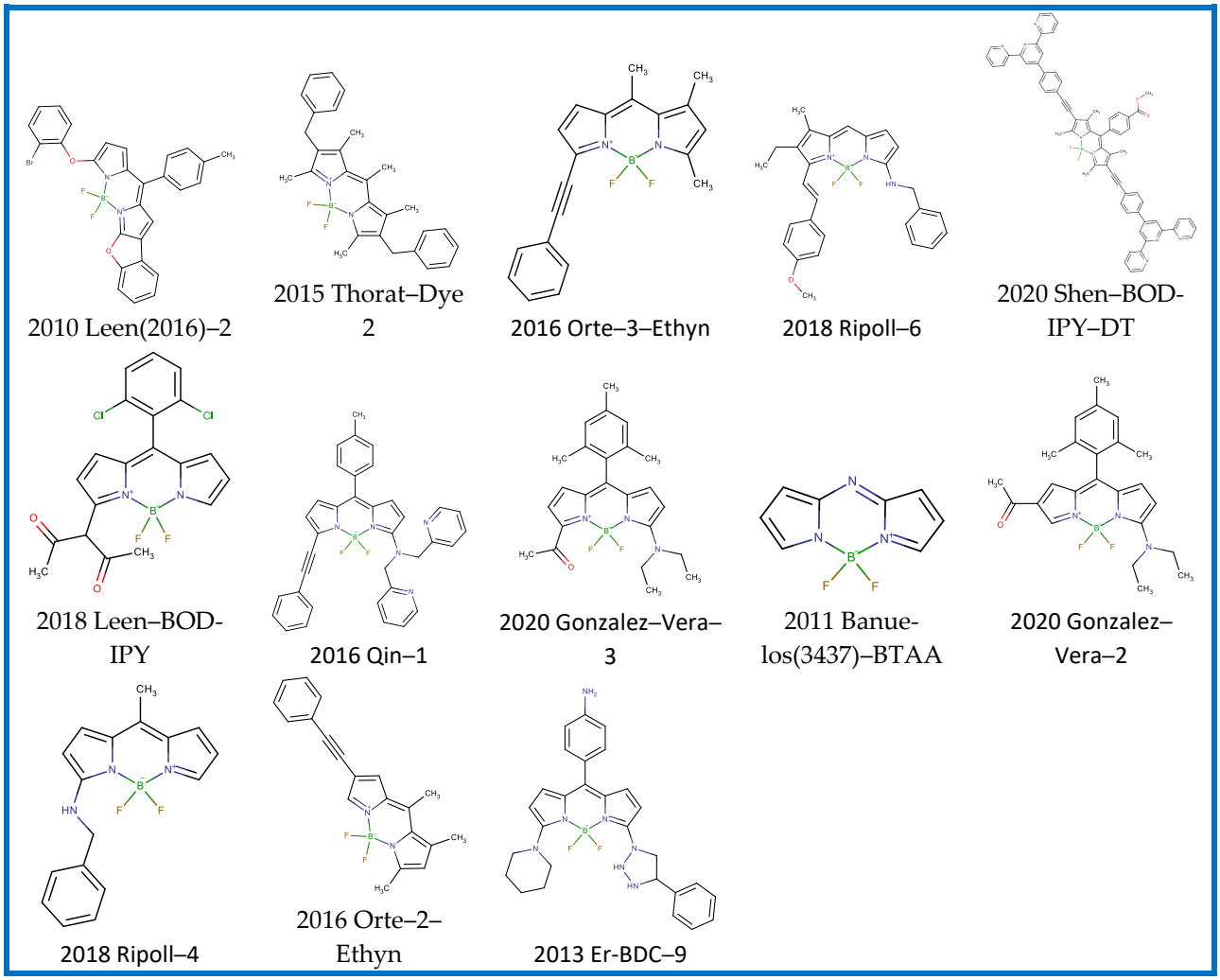

Scheme 6. Cluster 6; A: (−027)–(−1.25).

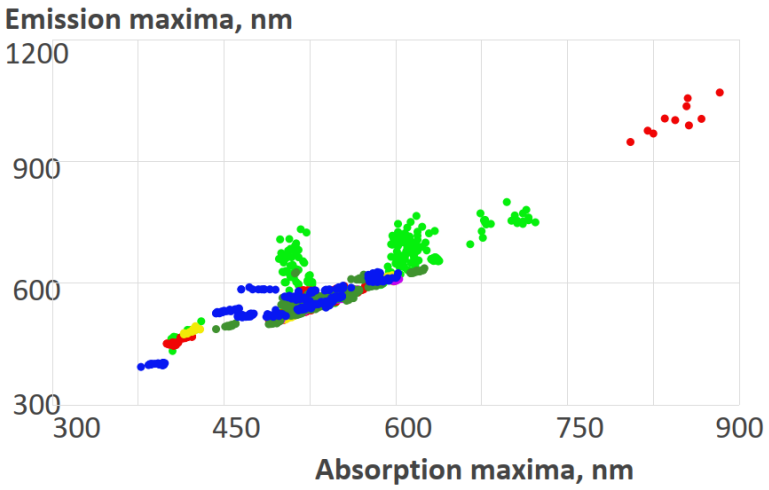

Figure 2. Absorption maxima versus emission maxima plot for a six-cluster dataset of 115 BODIPYs. For a key for the clusters, see in Schemes 1–6 and Figure 3.

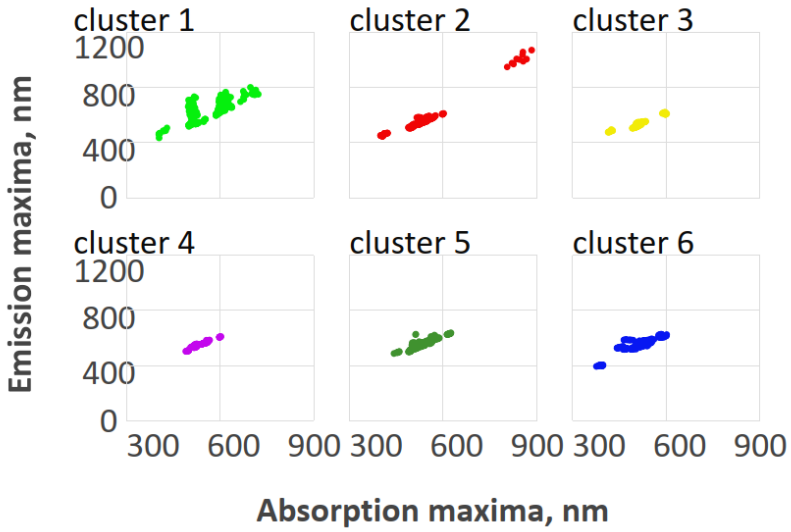

Figure 3. Absorption maxima versus emission maxima plot for a six-cluster dataset of 115 BODIPYs. For a key for the clusters, see in Schemes 1–6.

The clustering of the dyes according to solvatochromic sensitivity parameter A helps understand the general concept of the solvatochromic classification of the dyes. For instance, the plot for absorption maxima versus emission maxima for cluster 1 in Figures 2 and 3 exhibiting high positive solvatochromism depicts several vertically oriented asterisms with an approximately constant level of absorption in the solvents of a different nature, while the emission properties are varied in a wide range, indicating the high polarity of the molecule in the excited state. On the contrary, the absorption versus emission plot for cluster 6 demonstrates a wide variation in the absorption maxima and a low variation of emission characterizing the low polarity of the molecules in the excited state. Such behavior for the fluorophore is not typical. The increased values of the Stokes shift in cluster 1 in Figures 4 and 5 are shifted to the positive direction of the x-axis (less negative values), while those in cluster 6 to the opposite side follow the values of parameter A. If we take into consideration the other two pairs of symmetric clusters 2, 5, and 3, 4, shown in Figures 4 and 5, respectively, the characteristic behavior of the less polar dyes is similar to clusters 1 and 6, but not much more pronounced.

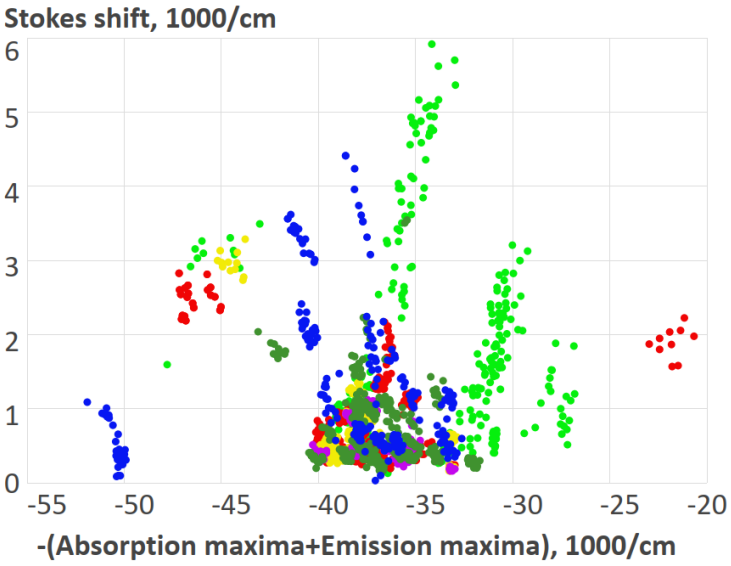

Figure 4. Stokes shift versus − (Absorption + Emission maxima) plot in terms of 1000/cm for a six-cluster dataset of 115 BODIPYs. For the key for the clusters, see Schemes 1–6 and Figure 3.

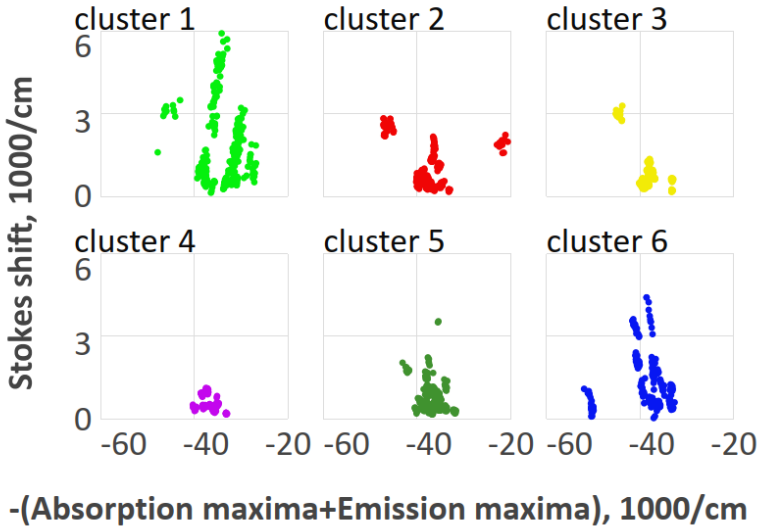

Figure 5. Stokes shift vs − (Absorption maxima + Emission maxima) diagram in terms of 1000/cm for a 6-cluster dataset of 115 BODIPYs. For the key for the clusters, see Schemes 1–6 and Figure 3.

The frequency diagram shown in Figure 6 demonstrates a high quantum yield for a large number of dyes bearing near-zero solvatochromism (clusters 4 and 5), indicating the role of the dye polarity in the quantum yield. The plot of toe quantum yield vs Stokes shift, shown in Figure 7, is convenient for practical use.

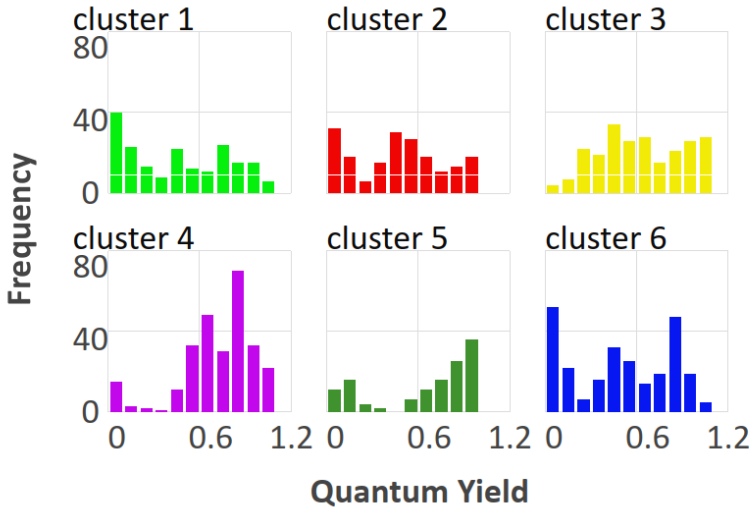

Figure 6. Frequency diagram for the quantum yield for a six-cluster dataset of 115 BODIPYs. The total frequency diagram for the quantum yield is shown in Figure 1d. For the key for the clusters, see Schemes 1–6.

2.2.2. 24-Cluster Dataset of High Solvatochromic Sensitivity

More detailed clustering of the dataset up to count 24 helps to identify the more regular behavior of the dyes in several clusters. The first one, the absorption maxima versus the emission maxima, is shown in Figure 8, for an approximate visualization of the absorption and the emission spectral range of the BODIPY fluorophores. Figure 8 illustrates the general semiempirical rule for the relationships between the absorption and emission wavenumbers approximated by Equation (4). Figure 9 clarifies the role of the relationship between the Stokes shift and − (Absorption maxima + Emission maxima) for polar sensors according to Equation (1). The plot of the quantum yield versus Stokes shift in Figure 10 supports understanding a common statement for polarity sensitive fluorophores—the decrease in quantum yield is accompanied by an increase in the Stokes shift.

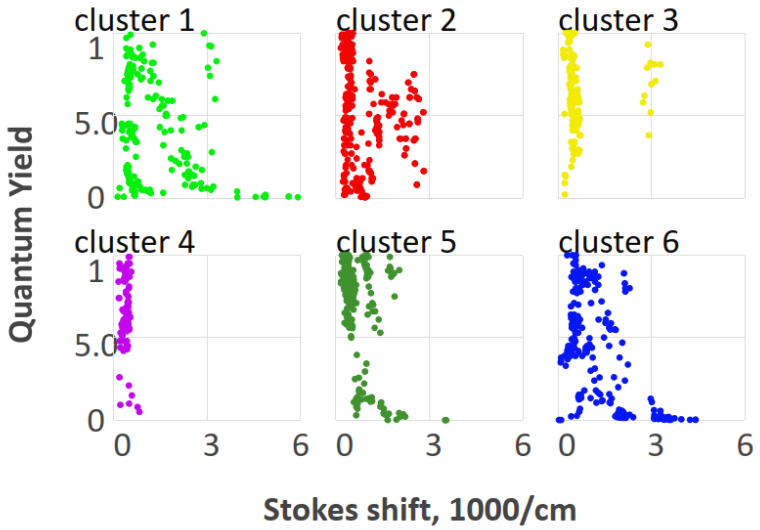

Figure 7. Quantum yield versus Stokes shift diagram for a six-cluster dataset of 115 BODIPYs. For a key for the clusters, see Schemes 1–6.

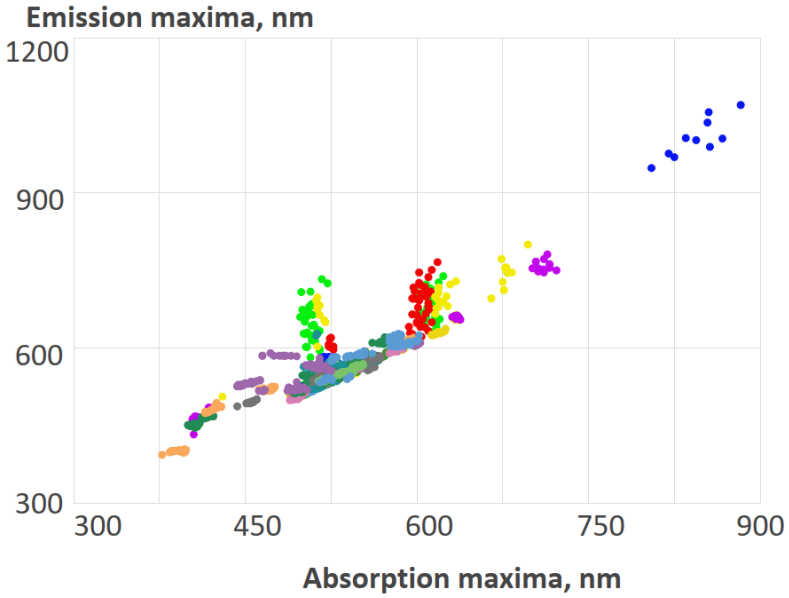

Figure 8. Absorption maxima versus emission maxima plot for a 24-cluster dataset of 115 BODIPYs. For the key for the clusters, see Figures 9 and 10.

The diagrams in Figures 9 and 10 (see in particular clusters 1–2 and 23–24) show regular behavior for dyes bearing a high positive and high negative solvatochromic sensitivity, respectively. Those fluorophores exhibiting a charge transfer in polar solvents are suitable for polarity mapping due to the high deviation in the absorption and emission wavelength, as well as the quantum yield and Stokes shift. The chemical structures of the corresponding dyes are shown below in Schemes 7 and 8. Several compounds in this multitude coincide with those estimated in chemoinformatics research based on the submolecular fragments approach [57].

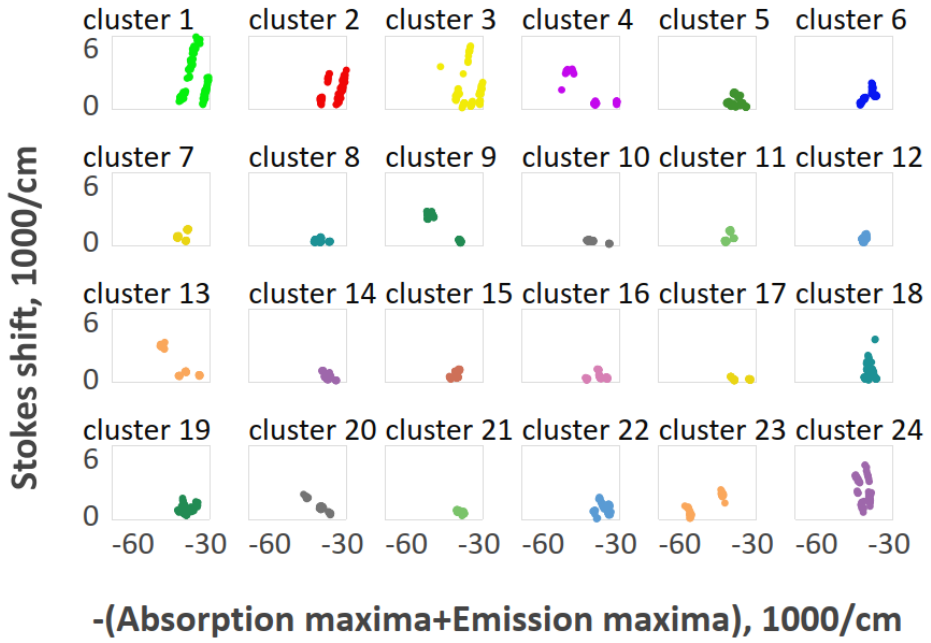

Figure 9. Stokes shift versus − (absorption maxima + emission maxima) diagram in terms of 1000/cm for a 24-cluster dataset of 115 BODIPYs, in decreased order, of parameter A.

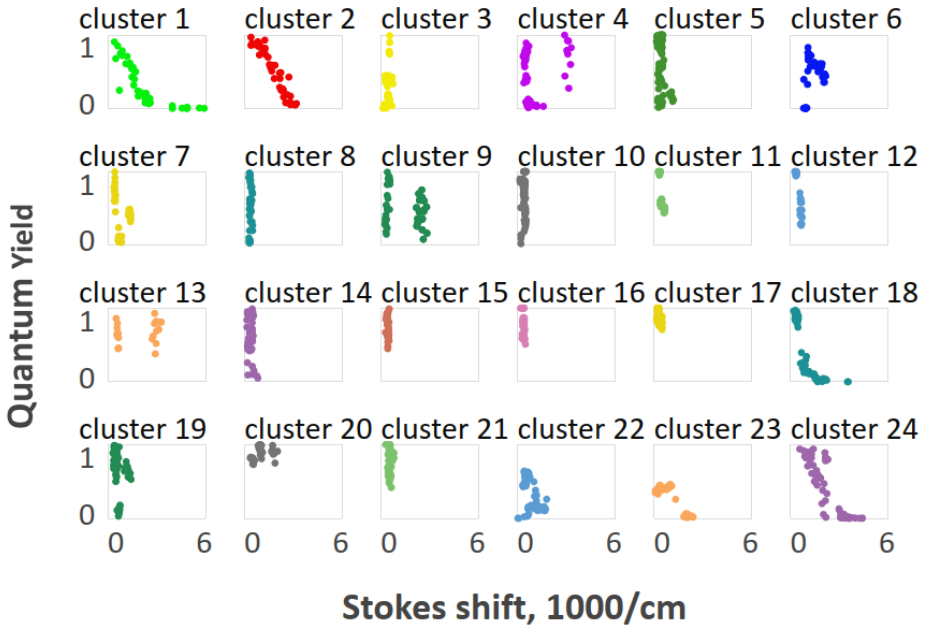

Figure 10. Quantum yield versus Stokes shift diagram in terms of 1000/cm for a 24-cluster dataset of 115 BODIPYs, in decreased order, of parameter A.

It is noteworthy that the diagram for quantum yield versus Stokes shift in Figure 10 for several dyes in clusters 1, 2, and 23, 24 could be approximated by one curve, respectively, while the plot for the Stokes shift versus − (absorption maxima + emission maxima) for the correspondent clusters in Figure 9 could be approximated by two lines. As an exception, a slight increase in the quantum yield versus Stokes shift is exhibited for parent aza-BODIPY, 2011 Banuelos(3437)-BTAA [69], which is provided in the dataset for comparison with the dipyrrin dyes. A similar behavior is demonstrated by 2018 Leen-BODIPY [93] in cluster 22/24, which could be attributed to the keto-enol tautomerism of the diketone fragment of the molecule.

Cluster 1/24		
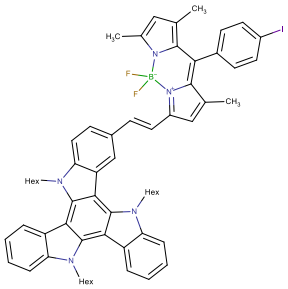	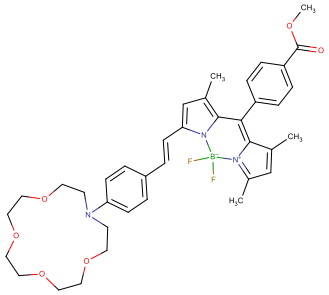	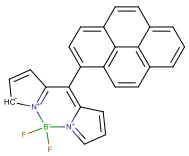
2013 Nano–TX(6); A: 1.18	2008 Qin–1; A: 0.91	2015 Caltagirone–Py–BODIPY; A: 1.02
Cluster 2/24		
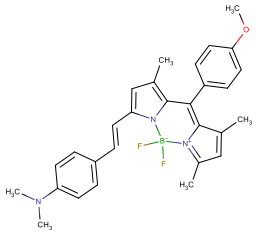	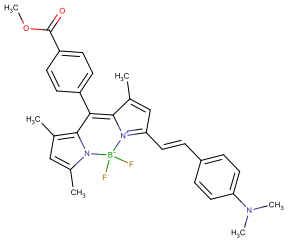	
2006 Baruah–1; A: 0.85	2010 Filarowski–1; A: 0.88	

Scheme 7. Chemical structures of dyes in clusters 1/24 and 2/24, bearing a high positive solvatochromism.

Cluster 23/24	
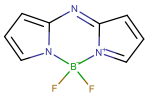	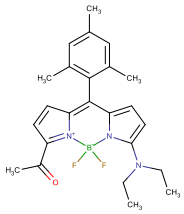
2011 Banuelos(3437)–BTAA; A: −0.58	2020 Gonzalez–Vera–3; A: −0.54

Cluster 24/24			
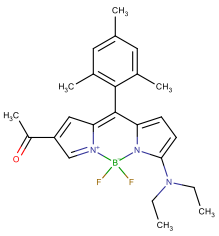	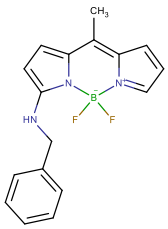	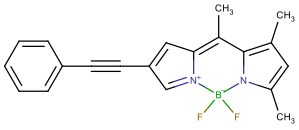	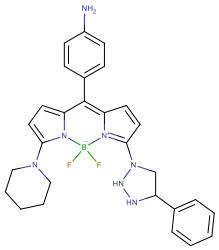
2020 Gonzalez–Vera–2; A: −0.67	2018 Ripoll–4; A: −0.80	2016 Orte–2–Ethyn; A: −1.21	2013 Er–BDC–9; A: −1.25

Scheme 8. Chemical structures of dyes in clusters 23/24 and 24/24, bearing a high negative solvatochromism.

2.2.3. BODIPYs Bearing Near-Zero Solvatochromism

The diagrams in Figure 10 reveal several groups of dyes exhibiting near-zero solvatochromic sensitivity. Several dyes in cluster 18 bearing near-zero solvatochromism form a single group approximating the relationship of quantum yield versus Stokes shift in a wide range of Stokes shift for fluorescence emission within 530–630 nm. The dyes are shown in Scheme 9.

Cluster 18/24

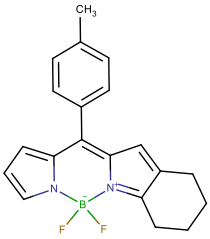

2012 Boens(9621)–5;
A: −0.16

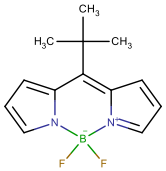

2015 Jiao–2;
A: −0.17

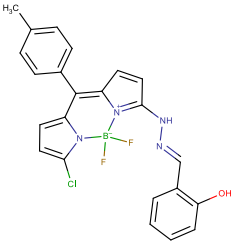

2015 Filarowski–A;
A: −0.18

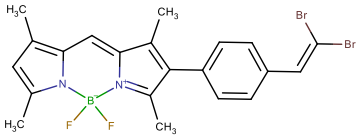

2019 Ali–16;
A: −0.18

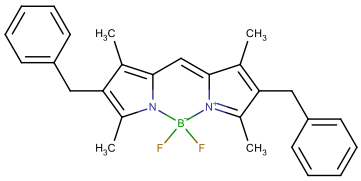

2015 Thorat–Dye 4;
A: −0.18

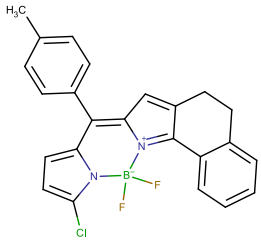

2012 Boens(9621)–3;
A: −0.18

Scheme 9. Chemical structures of the dyes in clusters 18/24 bearing near zero solvatochromism.

The individual dyes covering a wide range of quantum yields are exemplified by the following compounds shown in Scheme 10.

The above-mentioned members of clusters 7, 8, 9, 10, and 19 formed groups of dyes with quantum yields within 0.02–1 and Stokes shifts within 170–860 cm^{-1}, 1270–1400 cm^{-1}, and 2190–2800 cm^{-1}.

Several dyes mentioned above in this section exhibited molecular rotor effects, for example, those in clusters 7a, 9a, 9b, and 19. The dye in cluster 7 is known to exhibit a high quantum yield in solvents with a high polarity. This observation demonstrates the applicability of the developed tool for selecting efficient fluorophores demonstrating a low spectral sensitivity and high sensitivity of quantum yield to the polar solvents.

2.3. Analysis of Duplicates and Evaluation of Deviations of Spectral Data

A new tool for selecting the fluorescent probes proposed above is convenient for the analysis of deviation of experimental data for identical compounds. In essence, the problem of duplicates in chemoinformatics is solved by special algorithms based on, for example, SMILES or IUPAC InChI formats [107]. Normally, duplicate chemical structures are deleted from the dataset. However, spectral data for the essayed repeated compounds, as well as their solvatochromic sensitivity, could be used for evaluating the deviation of the correspondent properties in various experiments.

Cluster 7a/24; A: 0.07–0.06		Cluster 7b/24; A: 0.07–0.06	Cluster 8/24; A: 0.05–0.02	
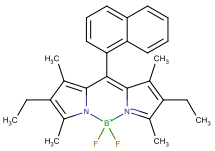	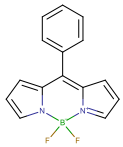	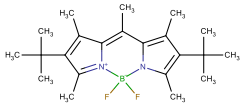	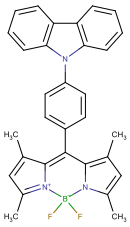	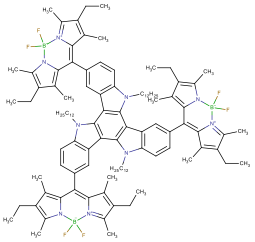
2016 Marfin(1975)–2	2016 Orte–8–Ph	2004 Banuelos–Prieto(5503)–PM597	2016 Telore–7a	2017 Sadak–15
Cluster 9a/24; A: 0.02–0.01			Cluster 9b/24; A: 0.02–0.01	
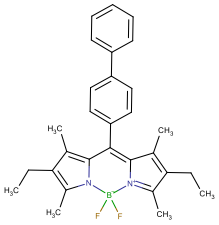	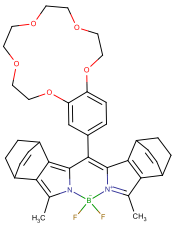		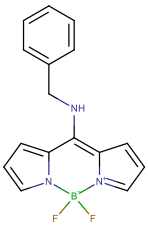	
2016 Marfin(1975)–5	2004 Shen–3d		2014 Boens–8; 2018 Ripoll–2	
Cluster 10/24; A: 0.01			Cluster 19/24; A: (−0.18)–(−0.2)	
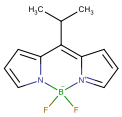	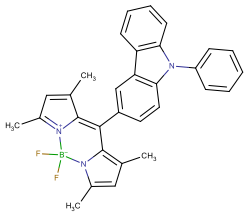	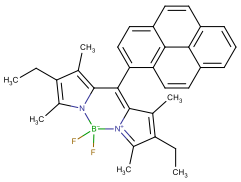	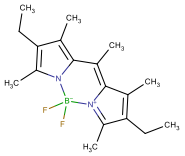	
2015 Jiao–5	2016 Telore–7	2016 Marfin(1975)–4	1998 Lopez–Arbeloa–PM567	
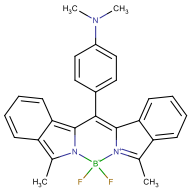		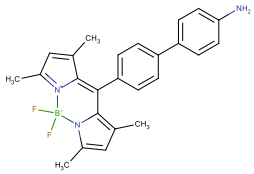		
2004 Shen–4b		2016 Gupta–1		

Scheme 10. Chemical structures of the dyes in clusters 7/24, 8/24, 9/24, 10/24, and 19/24 bearing near zero solvatochromism.

The chemical structures of the duplicates of the dataset collected in the current research are represented in Scheme 11. The deviation of the solvatochromic sensitivity parameter A for each duplicate is shown in Figures 11 and 12. The solvent count is shown above each column. All of the cases with a solvent count equal to or above 10 correspond to the dataset in Table 1, while a solvent count below 10 corresponds to the extra dataset of duplicates shown in Table 2, which were collected from the literature for a comparison of the spectral data.

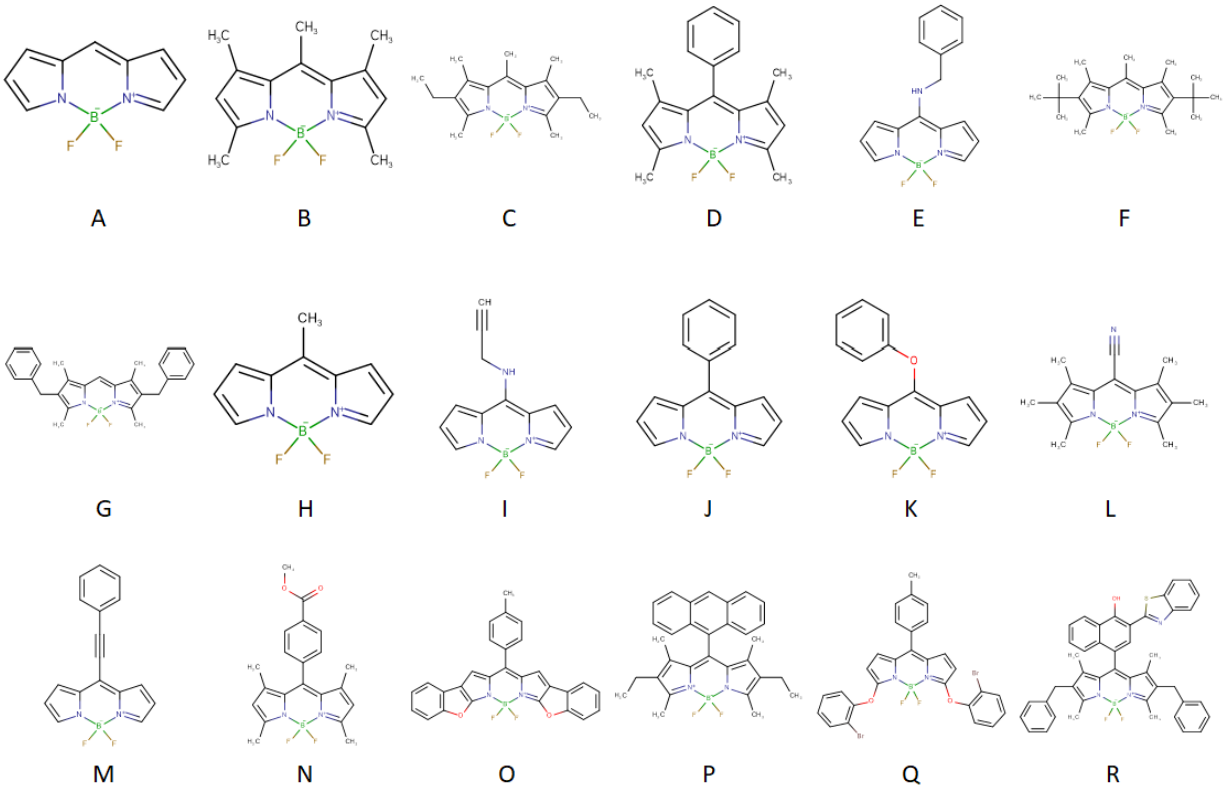

Scheme 11. Chemical structure of the duplicates of the target dataset studied in the current research.

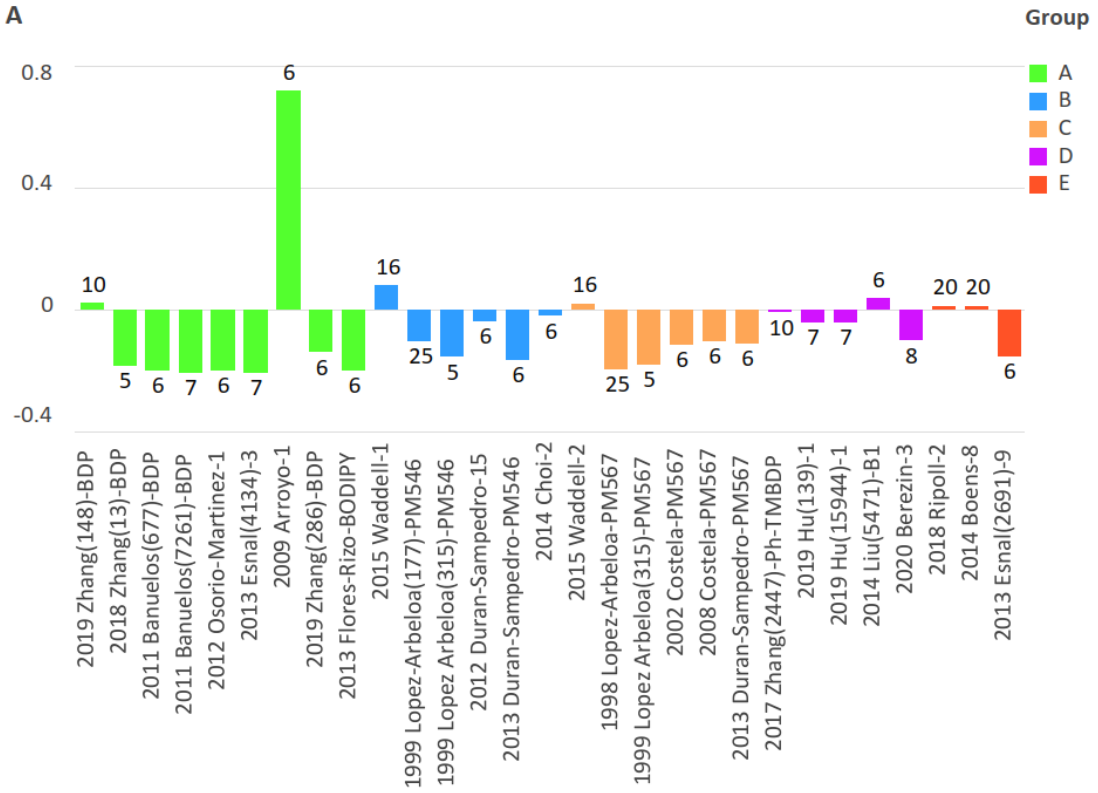

Figure 11. Solvatochromic sensitivity parameter A for the duplicates of the studied dataset, solvent count $\geq$ 10 for a target dataset, and solvent count $\leq$ 9 for an extra dataset.

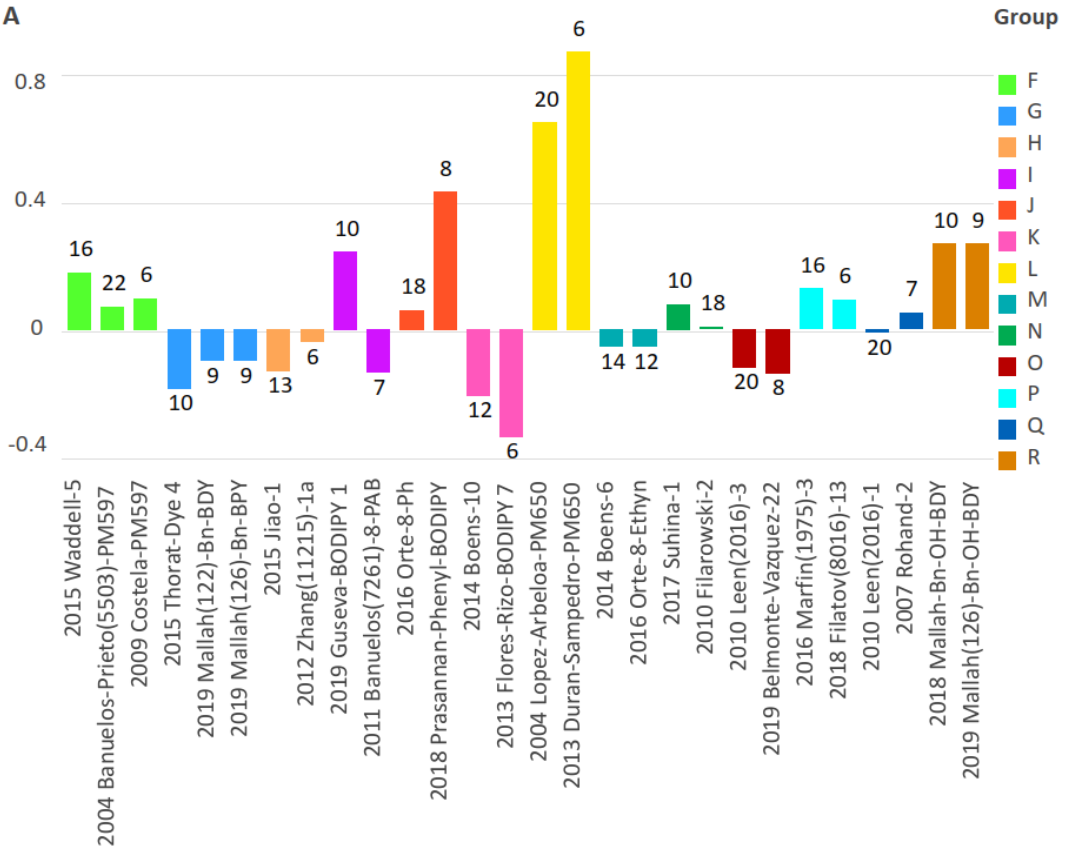

Figure 12. Solvatochromic sensitivity for duplicates of the studied dataset, solvent count $\geq$ 10 for the target dataset, and solvent count $\leq$ 9 for an extra dataset.

Table 2. List of dyes selected for a comparison of the duplicates.

List of Dyes	
1999 Lopez Arbeloa(315)–PM546 [108]	2013 Esnal(4134)–3 [121]
1999 Lopez Arbeloa(315)–PM567 [108]	2013 Flores–Rizo–BODIPY [122]
2002 Costela–PM567 [109]	2013 Flores–Rizo–BODIPY 7 [122]
2007 Rohand–2 [110]	2014 Choi–2 [123]
2008 Costela–PM567 [111]	2014 Liu(5471)–B1 [124]
2009 Arroyo–1 [112]	2018 Filatov(8016)–13 [125]
2009 Costela–PM597 [113]	2018 Prasannan–Phenyl–BODIPY [126]
2011 Banuelos(677)–BDP [114]	2018 Zhang(13)–BDP [127]
2011 Banuelos(7261)–8–PAB [115]	2019 Belmonte–Vazquez–22 [128]
2011 Banuelos(7261)–BDP [115]	2019 Hu(139)–1 [129]
2012 Duran-Sampedro–15 [116]	2019 Hu(15944)–1 [130]
2012 Osorio-Martinez–1 [117]	2019 Mallah(122)–Bn–BDY [131]
2012 Zhang(11215)–1a [118]	2019 Mallah(126)–Bn–BPY [132]
2013 Duran–Sampedro–PM546 [119]	2019 Mallah(126)–Bn–OH–BDY [132]
2013 Duran–Sampedro–PM567 [119]	2019 Zhang(286)–BDP [133]
2013 Duran–Sampedro–PM650 [119]	2020 Berezin–3 [134]
2013 Esnal(2691)–9 [120]	

The analysis of the solvatochromic sensitivity parameter A for all duplicates is a compact form of comparison of the data for solvatochromic behaviour compared with the whole spectral dataset. The solvatochromic sensitivity of the compounds of the groups G, M, N, O, P, Q, and R lies within the limits of the experimental error shown in the dataset represented in files of SI.csv and SI.sdf. However, several other compounds depict a high

deviation, for example, a parent compound 2009 Arroyo-1 in group A, 2015 Waddell-1, 2015 Waddell-2, and the compounds in groups I and J.

It is noteworthy that several duplicate compounds have been studied in a number of experiments for quite different solvents. For example, the dyes in group F demonstrate a similar solvatochromic sensitivity with a positive solvatochromism (A > 0) for a series of 16, 22, and 6 solvents.

According to the data in the diagram shown in Figure 1, the mean standard deviation SD and standard deviation of the mean SD/$\sqrt{n}$ for the solvatochromic sensitivity are estimated as follows, respectively: group A: (with an excluded extra value for 2009 Aroyo-1) 0.077, 0.037; group B: 0.091, 0.037; group C: 0.076, 0.031.

The above results could be clarified by a comparison of the spectral and photophysical data reported by different authors for each solvent. A few examples are shown for groups A, B, C, and D, respectively, in the figures, namely: SI_Figure S4-A-Em_vs_Abs, SI_Figure S4-A-Em_vs_Solvent, SI_Figure S4-B-Em_vs_Abs, SI_Figure S4-B-Em_vs_Solvent, SI_Figure S4-C-Em_vs_Abs, SI_Figure S4-C-Em_vs_Solvent, SI_Figure S4-D-Em_vs_Abs, and SI_Figure S4-D-Em_vs_Solvent (see Supplementary Information). The tooltip text for each mark in the figure demonstrates the compound ID, solvent name, solvatochromic sensitivity, relation E/C, absorption maxima, emission maxima, Stokes shift, and quantum yield.

3. Materials and Methods

3.1. Dataset of BODIPYs

The list of dyes included a total dataset of 115 BODIPYs and the corresponding references are shown above in Table 1 (Section 2.1). The dataset of BODIPY fluorophores collected in this study are listed in SI.csv and SI.sdf files with a correspondent count for solvents; references and IDs generated from the year of publication, first author, and title of the compound in the paper. The chemical structure in SMILES format and the direct code of JChem [107] was used for arranging the data. Each series of spectral and photophysical data are represented by 10–30 solvents for the analysis of the solvatochromic effect.

The chemical structures of the fluorophores are depicted in Schemes 1–6 in Section 2.2.1.

3.2. Evaluation of Statistical Deviations in Spectral and Photophysical Data

The dispersion of spectral data was evaluated through the use of duplicates in the dataset. For this purpose, additional data for spectral behaviour of BODIPYs covering six to nine solvents in each series, shown in Table 2 (Section 2.3) (see also Table S2 in Supplementary Information), were used along with software for the analysis and modelling of the molecular properties, such as DataWarrior [135] and ChemMine Tools [136].

3.3. Calculation of Solvatochromic Sensitivity of BODIPY Fluorophores

In previous research, a novel methodology was reported for studying the solvatochromism of BODIPYs [56,57]. This approach explores the empirical generalization of solvents' functions in Liptay's theory [137] of solvatochromism yielding an easy approach for treating a wide variety of spectral data published in the literature. The corresponding semiempirical equations are expressed as follows:

$$\nu(Abs) - \nu(Em) = -A[\nu(Abs) + \nu(Em)] + B \quad (1)$$

$$\nu(Abs) = \frac{1-A}{2}[\nu(Abs) + \nu(Em)] + \frac{B}{2} \quad (2)$$

$$\nu(Abs) = -C[\nu(Abs) + \nu(Em)] + D \quad (2a)$$

$$\nu(Em) = \frac{1+A}{2}[\nu(Abs) + \nu(Em)] - \frac{B}{2} \quad (3)$$

$$\nu(Em) = -E[\nu(Abs) + \nu(Em)] + F \quad (3a)$$

$$\nu(Em) = \frac{1+A}{1-A}\nu(Abs) - \frac{B}{1-A} \quad (4)$$

$$A = \frac{(\mu_e - \mu_g)^2}{\mu_e^2 - \mu_g^2} \quad (5)$$

where $\nu(Abs)$, $\nu(Em)$ is the wavenumbers that correspond to the absorption and emission maxima; A, B are the solvatochromic sensitivity coefficients, evaluated as regression coefficients of the linear approximation $\nu(Abs) - \nu(Em)$ vs $-[\nu(Abs) + \nu(Em)]$; and $\mu(g)$ and $\mu(e)$ are the vectors of the dipole moments of the fluorophore in the ground and excited states. For simplicity, the vector symbol is omitted.

Parameter A, described by Equation (5), is written in a more general form than in previous research [56,57] (see Supplementary Information). It helps to use dipole moments in vector form with no additional assumptions because the square of a vector function has a scalar value.

As far as parameter A is a function of dipole moments controlling the solvation of the fluorophore and dye spectral behavior in the ground and excited states, it is reasonable to use it as a quantitative measure of the solvatochromic sensitivity.

Coefficient A can be experimentally evaluated from the regression coefficients of Equations (1), (2a), and (3a).

The form of Equations (1), (2a), and (3a) is convenient for the simultaneous analysis of the behaviour of the three spectral functions, $\nu(Abs) - \nu(Em)$, $\nu(Abs)$, and $\nu(Em)$, shown in one plot (see Figures 13–15 below).

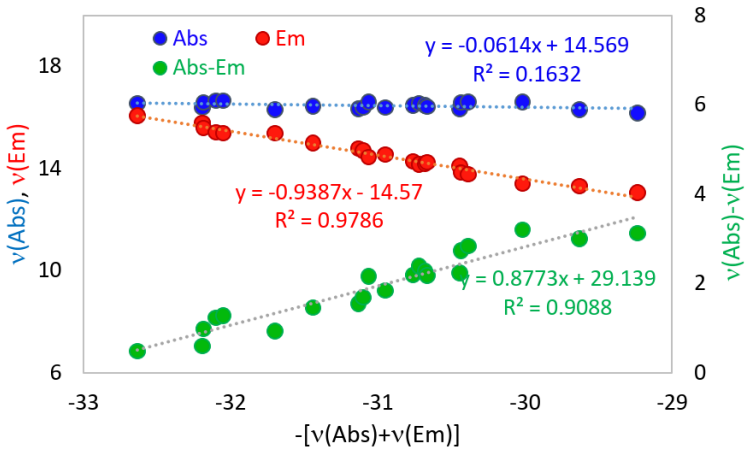

Figure 13. Relationships between the spectral properties of fluorophore 2010 Filarowski–1 in a series of solvents according to Equations (1)–(3): $A = 0.877$, $C = -0.061$, $E = -0.939$.

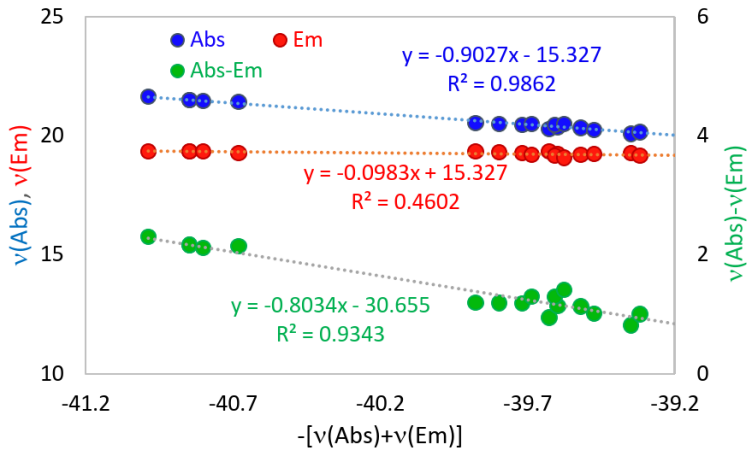

Figure 14. Relationships between the spectral properties of fluorophore 2018 Ripoll–4 in a series of solvents according to Equations (1)–(3): $A = -0.803$, $C = -0.903$, $E = -0.098$.

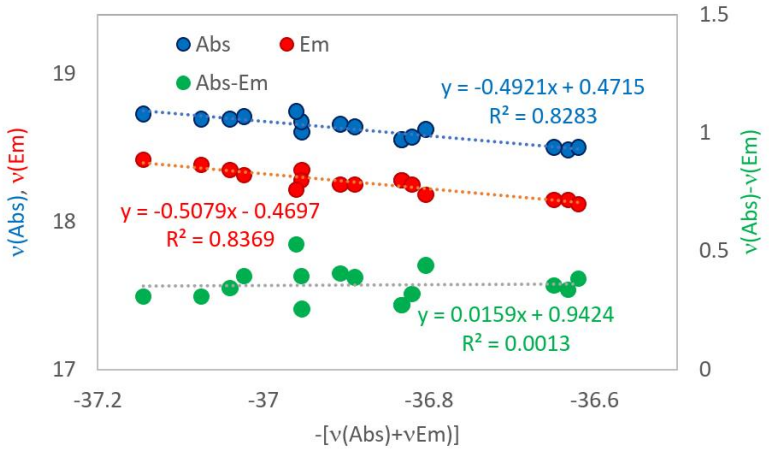

Figure 15. Relationships between the spectral properties of fluorophore 2016 Marfin(1975)–5 in a series of solvents according to Equations (1)–(3): $A = 0.016$, $C = -0.492$, $E = -0.508$.

A pairwise comparison of Equations (2) and (2a), and (3) and (3a) yields slopes C and E, respectively:

$$C = -\frac{1-A}{2};\ E = -\frac{1+A}{2} \tag{6}$$

Solvatochromic parameter A is estimated directly as the regression coefficient of Equation (1) for the Stokes shift or as the difference between C and E:

$$A = C - E \tag{7}$$

On the other hand, parameters C and E, defined by Equation (6), are suitable for estimating the relationship $\nu(Abs)$ vs $\nu(Em)$:

$$\frac{1+A}{1-A} = \frac{E}{C} \tag{8}$$

in order to apply Equation (4).

Expression (7) is useful for the measurement of the solvatochromic sensitivity of the relatively high positive and negative values, $A > 0$, $A < 0$, while the relation E/C, defined by Equation (8), is useful for characterising the near-zero solvatochromic sensitivity, $A \approx 0$, $E/C \approx 1$.

In the case of coplanarity of the vectors of the dipole moments $\mu(g)$ and $\mu(e)$, they can be used as scalar parameters, thus Expressions (5) and (8) are simplified for a clear understanding of the physicochemical meaning of parameter A defining the solvatochromic sensitivity:

$$A = \frac{\mu(e) - \mu(g)}{\mu(e) + \mu(g)},\ \frac{E}{C} = \frac{1+A}{1-A} = \frac{\mu(e)}{\mu(g)} \tag{9}$$

An illustration of the calculation method is provided in the papers [56,57]. Some additional examples are given below in Figures 13–15 for the fluorophores discussed above. In the case of high positive and negative solvatochromism (Figures 13 and 14), the Stokes shift exhibits a low statistical deviation from the linear correlation suitable for the estimation of parameter A; in the case of near-zero solvatochromism (Figure 15), the absorption or emission wavenumbers are more suitable for this purpose.

The experimentally evaluated parameters of Equations (1), (2a), (3a), (7), and (8), as well as their statistical characteristics for a dataset of 115 BODIPYs, are provided in the Supplementary Information.

3.4. Clustering the Properties of the Fluorophores and the Graphical Analysis

The clustering of the experimental data for a whole family of BODIPYs was performed by the parameters of solvatochromic sensitivity parameter A. This method of presentation helps to highlight each dye in a series of solvents, as well as to compare different series with a similar solvatochromic sensitivity. A graphical analysis of the spectral and photophysical properties of the collected BODIPYs was performed with the software Scimago Graphica [138].

4. Conclusions

Based on published results, a dataset of 115 BODIPY sensors in a series of 10–30 solvents with correspondent spectral and photophysical characteristics was collected. The solvatochromic sensitivity of each dye was evaluated by a recently developed semiempirical approach for the analysis of the solvatochromism. The polarity of the dyes was divided into 6 and 24 clusters from high negative to high positive levels, and was applied for the classification of fluorophores and an analysis of their properties.

The analysis of clusters combining several dyes in an individual series of solvents shows that dyes with a high polarity, with either a positive or negative solvatochromism, demonstrated regular changes in the absorption maxima versus emission maxima, Stokes shift versus − (absorption maxima + emission maxima), and quantum yield versus Stokes shift in a wide range of properties. Non-polar probes were arranged into characteristic clusters with quantum yields of 0.02–1 and Stokes shifts of 170–860 cm^{-1}, 1270–1400 cm^{-1}, and 2190–2800 cm^{-1}.

The developed tool based on the classification of solvatochromic sensitivity is suitable for the efficient selection of fluorescent probes, for both the polarity and viscosity sensing of biological tissue through the use of individual dyes and a set of dyes. The selected BODIPY probes could serve as pattern samples for the testing and design of the fluorophores.

Supplementary Materials: The following supporting information can be downloaded at: https://www.mdpi.com/article/10.3390/ijms24021217/s1, files SI—decr order A.csv, SI.xlsx, SI.sdf, SI.docx, SI_Figure S4-A-Em_vs_Abs, SI_Figure S4-A-Em_vs_Solvent, SI_Figure S4-B-Em_vs_Abs, SI_Figure S4-B-Em_vs_Solvent, SI_Figure S4-C-Em_vs_Abs, SI_Figure S4-C-Em_vs_Solvent, SI_Figure S4-D-Em_vs_Abs, SI_Figure S4-D-Em_vs_Solvent. Additional htm-files: SI_Figure 2, SI_Figure 3, SI_Figure 4, SI_Figure 5, SI_Figure 6, SI_Figure 7, SI_Figure 8, SI_Figure 9, and SI_Figure 10 are corresponding to figures in the text of the paper with tooltip text characterising the compound ID, solvent name, solvatochromic sensitivity, relation E/C, Absorption maxima, Emission maxima, Stokes shift, and Quantum yield [139–149].

Author Contributions: Conceptualization, F.Y.T. and Y.S.M.; methodology, F.Y.T.; software, F.Y.T.; validation, V.S.K., A.O.M. and R.G.A.; formal analysis, Y.S.M.; investigation, F.Y.T., V.S.K., A.O.M. and R.G.A.; resources, F.Y.T.; data curation, F.Y.T., V.S.K., A.O.M. and R.G.A.; writing—original draft preparation, F.Y.T., Y.S.M.; writing—review and editing, F.Y.T., Y.S.M.; visualization, F.Y.T., R.G.A.; supervision, Y.S.M.; project administration, Y.S.M.; funding acquisition, Y.S.M. All authors have read and agreed to the published version of the manuscript.

Funding: This work received financial support from the Ministry of Science and Higher Education of the Russian Federation (no. 075-15-2021-579).

Institutional Review Board Statement: Not applicable.

Informed Consent Statement: Not applicable.

Data Availability Statement: https://doi.org/10.6084/m9.figshare.21805410.v1.

Acknowledgments: The authors are grateful to ChemAxon (www.chemaxon.com) for providing an academic license for JChem for Office and to Citavi (www.citavi.com) for providing a license for the reference manager.

Conflicts of Interest: The authors declare no competing interest.

References

1. Valanciunaite, J.; Kempf, E.; Seki, H.; Danylchuk, D.I.; Peyriéras, N.; Niko, Y.; Klymchenko, A.S. Polarity Mapping of Cells and Embryos by Improved Fluorescent Solvatochromic Pyrene Probe. *Anal. Chem.* **2020**, *92*, 6512–6520. [CrossRef] [PubMed]
2. Li, L.; Xu, Y.; Chen, Y.; Zheng, J.; Zhang, J.; Li, R.; Wan, H.; Yin, J.; Yuan, Z.; Chen, H. A family of push-pull bio-probes for tracking lipid droplets in living cells with the detection of heterogeneity and polarity. *Anal. Chim. Acta* **2020**, *1096*, 166–173. [CrossRef] [PubMed]
3. Wang, J.; Boens, N.; Jiao, L.; Hao, E. Aromatic b-fused BODIPY dyes as promising near-infrared dyes. *Org. Biomol. Chem.* **2020**, *18*, 4135–4156. [CrossRef]
4. Li, G.; Li, J.; Otsuka, Y.; Zhang, S.; Takahashi, M.; Yamada, K. A BODIPY-Based Fluorogenic Probe for Specific Imaging of Lipid Droplets. *Materials* **2020**, *13*, 677. [CrossRef]
5. Liu, P.; Mu, X.; Zhang, X.-D.; Ming, D. The Near-Infrared-II Fluorophores and Advanced Microscopy Technologies Development and Application in Bioimaging. *Bioconjug. Chem.* **2020**, *31*, 260–275. [CrossRef] [PubMed]
6. Pal, K.; Dutta, T.; Koner, A.L. An Enumerated Outlook of Intracellular Micropolarity Using Solvatochromic Organic Fluorescent Probes. *ACS Omega* **2021**, *6*, 28–37. [CrossRef] [PubMed]
7. Dzyuba, S.V. BODIPY Dyes as Probes and Sensors to Study Amyloid-β-Related Processes. *Biosensors* **2020**, *10*, 192. [CrossRef]
8. Solomonov, A.V.; Marfin, Y.S.; Rumyantsev, E.V. Design and applications of dipyrrin-based fluorescent dyes and related organic luminophores: From individual compounds to supramolecular self-assembled systems. *Dyes Pigments* **2019**, *162*, 517–542. [CrossRef]
9. Huang, Y.; Zhang, Y.; Huo, F.; Wen, Y.; Yin, C. Design strategy and bioimaging of small organic molecule multicolor fluorescent probes. *Sci. China Chem.* **2020**, *63*, 1742–1755. [CrossRef]
10. Deng, P.; Xiao, F.; Wang, Z.; Jin, G. A Novel BODIPY Quaternary Ammonium Salt-Based Fluorescent Probe: Synthesis, Physical Properties, and Live-Cell Imaging. *Front. Chem.* **2021**, *9*, 89. [CrossRef]
11. Xiao, H.; Li, P.; Tang, B. Recent progresses in fluorescent probes for detection of polarity. *Coord. Chem. Rev.* **2021**, *427*, 213582. [CrossRef]
12. Jun, J.V.; Chenoweth, D.M.; Petersson, E.J. Rational design of small molecule fluorescent probes for biological applications. *Org. Biomol. Chem.* **2020**, *18*, 5747–5763. [CrossRef] [PubMed]
13. Colas, K.; Doloczki, S.; Posada Urrutia, M.; Dyrager, C. Prevalent Bioimaging Scaffolds: Synthesis, Photophysical Properties and Applications. *Eur. J. Org. Chem.* **2021**, *2021*, 2133–2144. [CrossRef]
14. Yin, J.; Huang, L.; Wu, L.; Li, J.; James, T.D.; Lin, W. Small molecule based fluorescent chemosensors for imaging the microenvironment within specific cellular regions. *Chem. Soc. Rev.* **2021**, *50*, 12098–12150. [CrossRef] [PubMed]
15. Demchenko, A.P. *Introduction to Fluorescence Sensing*; Springer International Publishing: Cham, Switzerland, 2020; ISBN 978-3-030-60154-6.
16. Bobrov, A.V.; Kishalova, M.V.; Merkushev, D.A.; Marfin, Y. BODIPY in matrices: Brief review. *J. Phys. Conf. Ser.* **2021**, *1822*, 12020. [CrossRef]
17. Martynov, V.I.; Pakhomov, A.A. BODIPY derivatives as fluorescent reporters of molecular activities in living cells. *Russ. Chem. Rev.* **2021**, *90*, 1213–1262. [CrossRef]
18. Wan, Z.; Yu, S.; Wang, Q.; Tobia, J.; Chen, H.; Li, Z.; Liu, X.; Zhang, Y. A BODIPY-Based Far-Red-Absorbing Fluorescent Probe for Hypochlorous Acid Imaging. *ChemPhotoChem* **2022**, *6*, e202100250. [CrossRef]
19. Ma, C.; Sun, W.; Xu, L.; Qian, Y.; Dai, J.; Zhong, G.; Hou, Y.; Liu, J.; Shen, B. A minireview of viscosity-sensitive fluorescent probes: Design and biological applications. *J. Mater. Chem. B* **2020**, *8*, 9642–9651. [CrossRef]
20. Kimura, R.; Kitakado, H.; Osuka, A.; Saito, S. Flapping Peryleneimide as a Fluorescent Viscosity Probe: Comparison with BODIPY and DCVJ Molecular Rotors. *BCSJ* **2020**, *93*, 1102–1106. [CrossRef]
21. Liu, X.; Chi, W.; Qiao, Q.; Kokate, S.V.; Cabrera, E.P.; Xu, Z.; Liu, X.; Chang, Y.-T. Molecular Mechanism of Viscosity Sensitivity in BODIPY Rotors and Application to Motion-Based Fluorescent Sensors. *ACS Sens.* **2020**, *5*, 731–739. [CrossRef]
22. Zhang, J.; He, B.; Hu, Y.; Alam, P.; Zhang, H.; Lam, J.W.Y.; Tang, B.Z. Stimuli-Responsive AIEgens. *Adv. Mater.* **2021**, *33*, e2008071. [CrossRef] [PubMed]
23. Suzuki, S.; Sasaki, S.; Sairi, A.S.; Iwai, R.; Tang, B.Z.; Konishi, G. Principles of Aggregation-Induced Emission: Design of Deactivation Pathways for Advanced AIEgens and Applications. *Angew. Chem. Int. Ed Engl.* **2020**, *59*, 9856–9867. [CrossRef] [PubMed]
24. Liu, Z.; Jiang, Z.; Yan, M.; Wang, X. Recent Progress of BODIPY Dyes with Aggregation-Induced Emission. *Front. Chem.* **2019**, *7*, 712. [CrossRef]
25. Filatov, M.A. Heavy-atom-free BODIPY photosensitizers with intersystem crossing mediated by intramolecular photoinduced electron transfer. *Org. Biomol. Chem.* **2020**, *18*, 10–27. [CrossRef] [PubMed]
26. Dong, Y.; Dick, B.; Zhao, J. Twisted Bodipy derivative as a heavy-atom-free triplet photosensitizer showing strong absorption of yellow light, intersystem crossing, and a high-energy long-lived triplet state. *Org. Lett.* **2020**, *22*, 5535. [CrossRef]
27. Chen, K.; Dong, Y.; Zhao, X.; Imran, M.; Tang, G.; Zhao, J.; Liu, Q. Bodipy Derivatives as Triplet Photosensitizers and the Related Intersystem Crossing Mechanisms. *Front. Chem.* **2019**, *7*, 821. [CrossRef]
28. Kand, D.; Liu, P.; Navarro, M.X.; Fischer, L.J.; Rousso-Noori, L.; Friedmann-Morvinski, D.; Winter, A.H.; Miller, E.W.; Weinstain, R. Water-Soluble BODIPY Photocages with Tunable Cellular Localization. *J. Am. Chem. Soc.* **2020**, *142*, 4970–4974. [CrossRef]

29. Shrestha, P.; Dissanayake, K.C.; Gehrmann, E.J.; Wijesooriya, C.S.; Mukhopadhyay, A.; Smith, E.A.; Winter, A.H. Efficient Far-Red/Near-IR Absorbing BODIPY Photocages by Blocking Unproductive Conical Intersections. *J. Am. Chem. Soc.* **2020**, *142*, 15505–15512. [CrossRef]
30. Singh, P.K.; Majumdar, P.; Singh, S.P. Advances in BODIPY photocleavable protecting groups. *Coord. Chem. Rev.* **2021**, *449*, 214193. [CrossRef]
31. Contreras-García, E.; Lozano, C.; García-Iriepa, C.; Marazzi, M.; Winter, A.H.; Torres, C.; Sampedro, D. Controlling Antimicrobial Activity of Quinolones Using Visible/NIR Light-Activated BODIPY Photocages. *Pharmaceutics* **2022**, *14*, 1070. [CrossRef]
32. Shrestha, P.; Mukhopadhyay, A.; Dissanayake, K.C.; Winter, A.H. Efficiency of Functional Group Caging with Second-Generation Green- and Red-Light-Labile BODIPY Photoremovable Protecting Groups. *J. Org. Chem.* **2022**, *87*, 14334–14341. [CrossRef] [PubMed]
33. Leng, J.; Lan, X.; Liu, S.; Jia, W.; Cheng, W.; Cheng, J.; Liu, Z. Synthesis and bioimaging of a BODIPY-based fluorescence quenching probe for Fe3. *RSC Adv.* **2022**, *12*, 21332–21339. [CrossRef] [PubMed]
34. Kubota, Y. BODIPY Dyes and Their Analogues. In *Progress in the Science of Functional Dyes*; Ooyama, Y., Yagi, S., Eds.; Springer: Singapore, 2021; pp. 119–220. ISBN 978-981-33-4391-7.
35. Lee, J.-S.; Kim, H.K.; Feng, S.; Vendrell, M.; Chang, Y.-T. Accelerating fluorescent sensor discovery: Unbiased screening of a diversity-oriented BODIPY library. *Chem. Commun.* **2011**, *47*, 2339–2341. [CrossRef]
36. Zhai, D.; Lee, S.-C.; Vendrell, M.; Leong, L.P.; Chang, Y.-T. Synthesis of a novel BODIPY library and its application in the discovery of a fructose sensor. *ACS Comb. Sci.* **2012**, *14*, 81–84. [CrossRef] [PubMed]
37. Er, J.C.; Tang, M.K.; Chia, C.G.; Liew, H.; Vendrell, M.; Chang, Y.-T. MegaStokes BODIPY-triazoles as environmentally sensitive turn-on fluorescent dyes. *Chem. Sci.* **2013**, *4*, 2168. [CrossRef]
38. Alamudi, S.H.; Satapathy, R.; Kim, J.; Su, D.; Ren, H.; Das, R.; Hu, L.; Alvarado-Martínez, E.; Lee, J.Y.; Hoppmann, C.; et al. Development of background-free tame fluorescent probes for intracellular live cell imaging. *Nat. Commun.* **2016**, *7*, 11964. [CrossRef] [PubMed]
39. Bittel, A.M.; Davis, A.M.; Wang, L.; Nederlof, M.A.; Escobedo, J.O.; Strongin, R.M.; Gibbs, S.L. Varied Length Stokes Shift BODIPY-Based Fluorophores for Multicolor Microscopy. *Sci. Rep.* **2018**, *8*, 4590. [CrossRef]
40. Bittel, A.M.; Saldivar, I.S.; Dolman, N.J.; Nan, X.; Gibbs, S.L. Superresolution microscopy with novel BODIPY-based fluorophores. *PLoS ONE* **2018**, *13*, e0206104. [CrossRef]
41. Lee, J.-S.; Kang, N.-Y.; Kim, Y.K.; Samanta, A.; Feng, S.; Kim, H.K.; Vendrell, M.; Park, J.H.; Chang, Y.-T. Synthesis of a BODIPY library and its application to the development of live cell glucagon imaging probe. *J. Am. Chem. Soc.* **2009**, *131*, 10077–10082. [CrossRef]
42. Su, D.; Teoh, C.L.; Kang, N.-Y.; Yu, X.; Sahu, S.; Chang, Y.-T. Synthesis and systematic evaluation of dark resonance energy transfer (DRET)-based library and its application in cell imaging. *Chem. Asian J.* **2015**, *10*, 581–585. [CrossRef]
43. Vendrell, M.; Krishna, G.G.; Ghosh, K.K.; Zhai, D.; Lee, J.-S.; Zhu, Q.; Yau, Y.H.; Shochat, S.G.; Kim, H.; Chung, J.; et al. Solid-phase synthesis of BODIPY dyes and development of an immunoglobulin fluorescent sensor. *Chem. Commun.* **2011**, *47*, 8424–8426. [CrossRef] [PubMed]
44. Joung, J.F.; Han, M.; Jeong, M.; Park, S. Experimental database of optical properties of organic compounds. *Sci. Data* **2020**, *7*, 295. [CrossRef] [PubMed]
45. Joung, J.F.; Han, M.; Hwang, J.; Jeong, M.; Choi, D.H.; Park, S. Deep Learning Optical Spectroscopy Based on Experimental Database: Potential Applications to Molecular Design. *JACS Au* **2021**, *1*, 427–438. [CrossRef] [PubMed]
46. Ju, C.-W.; Bai, H.; Li, B.; Liu, R. Machine Learning Enables Highly Accurate Predictions of Photophysical Properties of Organic Fluorescent Materials: Emission Wavelengths and Quantum Yields. *J. Chem. Inf. Model.* **2021**, *61*, 1053–1065. [CrossRef]
47. Ye, Z.-R.; Huang, I.-S.; Chan, Y.-T.; Li, Z.-J.; Liao, C.-C.; Tsai, H.-R.; Hsieh, M.-C.; Chang, C.-C.; Tsai, M.-K. Predicting the emission wavelength of organic molecules using a combinatorial QSAR and machine learning approach. *RSC Adv.* **2020**, *10*, 23834–23841. [CrossRef]
48. Lin, Z.; Kohn, A.W.; van Voorhis, T. Toward Prediction of Nonradiative Decay Pathways in Organic Compounds II: Two Internal Conversion Channels in BODIPYs. *J. Phys. Chem. C* **2020**, *124*, 3925–3938. [CrossRef]
49. Matarranz, B.; Fernández, G. BODIPY dyes: Versatile building blocks to construct multiple types of self-assembled structures. *Chem. Phys. Rev.* **2021**, *2*, 41304. [CrossRef]
50. López Arbeloa, F.; Bañuelos Prieto, J.; Martínez Martínez, V.; Arbeloa López, T.; López Arbeloa, I. Intramolecular charge transfer in pyrromethene laser dyes: Photophysical behaviour of PM650. *Chemphyschem* **2004**, *5*, 1762–1771. [CrossRef]
51. Qin, W.; Baruah, M.; Sliwa, M.; van der Auweraer, M.; Borggraeve, W.M.D.; Beljonne, D.; van Averbeke, B.; Boens, N. Ratiometric, fluorescent BODIPY dye with aza crown ether functionality: Synthesis, solvatochromism, and metal ion complex formation. *J. Phys. Chem. A* **2008**, *112*, 6104–6114. [CrossRef]
52. Qin, W.; Dou, W.; Leen, V.; Dehaen, W.; van der Auweraer, M.; Boens, N. A ratiometric, fluorescent BODIPY-based probe for transition and heavy metal ions. *RSC Adv.* **2016**, *6*, 7806–7816. [CrossRef]
53. Orte, A.; Debroye, E.; Ruedas-Rama, M.J.; Garcia-Fernandez, E.; Robinson, D.; Crovetto, L.; Talavera, E.M.; Alvarez-Pez, J.M.; Leen, V.; Verbelen, B.; et al. Effect of the substitution position (2, 3 or 8) on the spectroscopic and photophysical properties of BODIPY dyes with a phenyl, styryl or phenylethynyl group. *RSC Adv.* **2016**, *6*, 102899–102913. [CrossRef]

54. Filarowski, A.; Kluba, M.; Cieślik-Boczula, K.; Koll, A.; Kochel, A.; Pandey, L.; Borggraeve, W.M.D.; van der Auweraer, M.; Catalán, J.; Boens, N. Generalized solvent scales as a tool for investigating solvent dependence of spectroscopic and kinetic parameters. Application to fluorescent BODIPY dyes. *Photochem. Photobiol. Sci.* **2010**, *9*, 996–1008. [CrossRef] [PubMed]
55. Ooyama, Y.; Yagi, S. (Eds.) *Progress in the Science of Functional Dyes*; Springer: Singapore, 2021; ISBN 978-981-33-4391-7.
56. Telegin, F.Y.; Marfin, Y.S. New insights into quantifying the solvatochromism of BODIPY based fluorescent probes. *Spectrochim. Acta A Mol. Biomol. Spectrosc.* **2021**, *255*, 119683. [CrossRef] [PubMed]
57. Telegin, F.Y.; Marfin, Y.S. Polarity and Structure of BODIPYs: A Semiempirical and Chemoinformation Analysis. *Russ. J. Inorg. Chem.* **2022**, *67*, 362–374. [CrossRef]
58. López Arbeloa, F.; López Arbeloa, T.; López Arbeloa, I.; García-Moreno, I.; Costela, A.; Sastre, R.; Amat-Guerri, F. Photophysical and lasing properties of pyrromethene567 dye in liquid solution: Environment effects. *Chem. Phys.* **1998**, *236*, 331–341. [CrossRef]
59. López Arbeloa, F.; López Arbeloa, T.; López Arbeloa, I. Electronic spectroscopy of pyrromethene 546. *J. Photochem. Photobiol. A Chem.* **1999**, *121*, 177–182. [CrossRef]
60. Bañuelos Prieto, J.; López Arbeloa, F.; Martinez Martinez, V.; Arbeloa López, T.; Amat-Guerri, F.; Liras, M.; López Arbeloa, I. Photophysical properties of a new 8-phenyl analogue of the laser dye PM567 in different solvents: Internal conversion mechanisms. *Chem. Phys. Lett.* **2004**, *385*, 29–35. [CrossRef]
61. Bañuelos Prieto, J.; López Arbeloa, F.; Martínez Martínez, V.; Arbeloa López, T.; López Arbeloa, I. Photophysical Properties of the Pyrromethene 597 Dye: Solvent Effect. *J. Phys. Chem. A* **2004**, *108*, 5503–5508. [CrossRef]
62. Shen, Z.; Röhr, H.; Rurack, K.; Uno, H.; Spieles, M.; Schulz, B.; Reck, G.; Ono, N. Boron-diindomethene (BDI) dyes and their tetrahydrobicyclo precursors–en route to a new class of highly emissive fluorophores for the red spectral range. *Chemistry* **2004**, *10*, 4853–4871. [CrossRef]
63. Baruah, M.; Qin, W.; Flors, C.; Hofkens, J.; Vallée, R.A.L.; Beljonne, D.; van der Auweraer, M.; Borggraeve, W.M.D.; Boens, N. Solvent and pH dependent fluorescent properties of a dimethylaminostyryl borondipyrromethene dye in solution. *J. Phys. Chem. A* **2006**, *110*, 5998–6009. [CrossRef]
64. Qin, W.; Baruah, M.; Borggraeve, W.M.D.; Boens, N. Photophysical properties of an on/off fluorescent pH indicator excitable with visible light based on a borondipyrromethene-linked phenol. *J. Photochem. Photobiol. A Chem.* **2006**, *183*, 190–197. [CrossRef]
65. Cieślik-Boczula, K.; Burgess, K.; Li, L.; Nguyen, B.; Pandey, L.; Borggraeve, W.M.D.; van der Auweraer, M.; Boens, N. Photophysics and stability of cyano-substituted boradiazaindacene dyes. *Photochem. Photobiol. Sci.* **2009**, *8*, 1006–1015. [CrossRef] [PubMed]
66. Qin, W.; Leen, V.; Dehaen, W.; Cui, J.; Xu, C.; Tang, X.; Liu, W.; Rohand, T.; Beljonne, D.; van Averbeke, B.; et al. 3,5-Dianilino Substituted Difluoroboron Dipyrromethene: Synthesis, Spectroscopy, Photophysics, Crystal Structure, Electrochemistry, and Quantum-Chemical Calculations †. *J. Phys. Chem. C* **2009**, *113*, 11731–11740. [CrossRef]
67. Chaudhuri, T.; Mula, S.; Chattopadhyay, S.; Banerjee, M. Photophysical properties of the 8-phenyl analogue of PM567: A theoretical rationalization. *Spectrochim. Acta A Mol. Biomol. Spectrosc.* **2010**, *75*, 739–744. [CrossRef]
68. Leen, V.; Qin, W.; Yang, W.; Cui, J.; Xu, C.; Tang, X.; Liu, W.; Robeyns, K.; van Meervelt, L.; Beljonne, D.; et al. Synthesis, spectroscopy, crystal structure determination, and quantum chemical calculations of BODIPY dyes with increasing conformational restriction and concomitant red-shifted visible absorption and fluorescence spectra. *Chem. Asian J.* **2010**, *5*, 2016–2026. [CrossRef] [PubMed]
69. Bañuelos, J.; Arbeloa, F.L.; Martinez, V.; Liras, M.; Costela, A.; Moreno, I.G.; Arbeloa, I.L. Difluoro-boron-triaza-anthracene: A laser dye in the blue region. Theoretical simulation of alternative difluoro-boron-diaza-aromatic systems. *Phys. Chem. Chem. Phys.* **2011**, *13*, 3437–3445. [CrossRef] [PubMed]
70. Boens, N.; Leen, V.; Dehaen, W.; Wang, L.; Robeyns, K.; Qin, W.; Tang, X.; Beljonne, D.; Tonnelé, C.; Paredes, J.M.; et al. Visible absorption and fluorescence spectroscopy of conformationally constrained, annulated BODIPY dyes. *J. Phys. Chem. A* **2012**, *116*, 9621–9631. [CrossRef]
71. Yin, Z.; Tam, A.Y.-Y.; Wong, K.M.-C.; Tao, C.-H.; Li, B.; Poon, C.-T.; Wu, L.; Yam, V.W.-W. Functionalized BODIPY with various sensory units–a versatile colorimetric and luminescent probe for pH and ions. *Dalton Trans.* **2012**, *41*, 11340–11350. [CrossRef]
72. Zhao, C.; Feng, P.; Cao, J.; Zhang, Y.; Wang, X.; Yang, Y.; Zhang, Y.; Zhang, J. 6-Hydroxyindole-based borondipyrromethene: Synthesis and spectroscopic studies. *Org. Biomol. Chem.* **2012**, *10*, 267–272. [CrossRef]
73. Nano, A.; Ziessel, R.; Stachelek, P.; Harriman, A. Charge-recombination fluorescence from push-pull electronic systems constructed around amino-substituted styryl-BODIPY dyes. *Chemistry* **2013**, *19*, 13528–13537. [CrossRef]
74. Yang, Y.; Zhang, L.; Li, B.; Zhang, L.; Liu, X. Triphenylamine-cored tetramethyl-BODIPY dyes: Synthesis, photophysics and lasing properties in organic media. *RSC Adv.* **2013**, *3*, 14993. [CrossRef]
75. Boens, N.; Wang, L.; Leen, V.; Yuan, P.; Verbelen, B.; Dehaen, W.; van der Auweraer, M.; Borggraeve, W.D.D.; van Meervelt, L.; Jacobs, J.; et al. 8-HaloBODIPYs and their 8-(C, N, O, S) substituted analogues: Solvent Dependent UV–Vis Spectroscopy, Variable Temperature NMR, Crystal Structure Determination, and Quantum Chemical Calculations. *J. Phys. Chem. A* **2014**, *118*, 1576–1594. [CrossRef] [PubMed]
76. Caltagirone, C.; Arca, M.; Falchi, A.M.; Lippolis, V.; Meli, V.; Monduzzi, M.; Nylander, T.; Rosa, A.; Schmidt, J.; Talmon, Y.; et al. Solvatochromic fluorescent BODIPY derivative as imaging agent in camptothecin loaded hexosomes for possible theranostic applications. *RSC Adv.* **2015**, *5*, 23443–23449. [CrossRef]

77. Feng, H.-T.; Xiong, J.-B.; Zheng, Y.-S.; Pan, B.; Zhang, C.; Wang, L.; Xie, Y. Multicolor Emissions by the Synergism of Intra/Intermolecular Slipped π–π Stackings of Tetraphenylethylene-DiBODIPY Conjugate. *Chem. Mater.* **2015**, *27*, 7812–7819. [CrossRef]
78. Filarowski, A.; Lopatkova, M.; Lipkowski, P.; van der Auweraer, M.; Leen, V.; Dehaen, W. Solvatochromism of BODIPY-Schiff dye. *J. Phys. Chem. B* **2015**, *119*, 2576–2584. [CrossRef] [PubMed]
79. Jiao, L.; Yu, C.; Wang, J.; Briggs, E.A.; Besley, N.A.; Robinson, D.; Ruedas-Rama, M.J.; Orte, A.; Crovetto, L.; Talavera, E.M.; et al. Unusual spectroscopic and photophysical properties of meso-tert-butylBODIPY in comparison to related alkylated BODIPY dyes. *RSC Adv.* **2015**, *5*, 89375–89388. [CrossRef]
80. Thorat, K.G.; Kamble, P.; Mallah, R.; Ray, A.K.; Sekar, N. Congeners of Pyrromethene-567 Dye: Perspectives from Synthesis, Photophysics, Photostability, Laser, and TD-DFT Theory. *J. Org. Chem.* **2015**, *80*, 6152–6164. [CrossRef]
81. Waddell, P.G.; Liu, X.; Zhao, T.; Cole, J.M. Rationalizing the photophysical properties of BODIPY laser dyes via aromaticity and electron-donor-based structural perturbations. *Dyes Pigments* **2015**, *116*, 74–81. [CrossRef]
82. Bacalum, M.; Wang, L.; Boodts, S.; Yuan, P.; Leen, V.; Smisdom, N.; Fron, E.; Knippenberg, S.; Fabre, G.; Trouillas, P.; et al. A Blue-Light-Emitting BODIPY Probe for Lipid Membranes. *Langmuir* **2016**, *32*, 3495–3505. [CrossRef]
83. Gupta, N.; Reja, S.I.; Bhalla, V.; Gupta, M.; Kaur, G.; Kumar, M. A bodipy based fluorescent probe for evaluating and identifying cancer, normal and apoptotic C6 cells on the basis of changes in intracellular viscosity. *J. Mater. Chem. B* **2016**, *4*, 1968–1977. [CrossRef]
84. Marfin, Y.S.; Vodyanova, O.S.; Merkushev, D.A.; Usoltsev, S.D.; Kurzin, V.O.; Rumyantsev, E.V. Effect of π-Extended Substituents on Photophysical Properties of BODIPY Dyes in Solutions. *J. Fluoresc.* **2016**, *26*, 1975–1985. [CrossRef] [PubMed]
85. Telore, R.D.; Jadhav, A.G.; Sekar, N. NLOphoric and solid state emissive BODIPY dyes containing N -phenylcarbazole core at meso position—Synthesis, photophysical properties of and DFT studies. *J. Lumin.* **2016**, *179*, 420–428. [CrossRef]
86. Vu, T.T.; Méallet-Renault, R.; Clavier, G.; Trofimov, B.A.; Kuimova, M.K. Tuning BODIPY molecular rotors into the red: Sensitivity to viscosity vs. temperature. *J. Mater. Chem. C* **2016**, *4*, 2828–2833. [CrossRef]
87. Zhu, H.; Fan, J.; Mu, H.; Zhu, T.; Zhang, Z.; Du, J.; Peng, X. d-PET-controlled "off-on" Polarity-sensitive Probes for Reporting Local Hydrophilicity within Lysosomes. *Sci. Rep.* **2016**, *6*, 35627. [CrossRef] [PubMed]
88. Petrushenko, K.B.; Petrushenko, I.K.; Petrova, O.V.; Sobenina, L.N.; Trofimov, B.A. Novel environment-sensitive 8-CF3 -BODIPY dye with 4-(dimethylamino)phenyl group at the 3-position: Synthesis and optical properties. *Dyes Pigments* **2017**, *136*, 488–495. [CrossRef]
89. Sadak, A.E.; Gören, A.C.; Bozdemir, Ö.A.; Saraçoğlu, N. Synthesis of Novel meso- Indole- and meso-Triazatruxene-BODIPY Dyes. *ChemistrySelect* **2017**, *2*, 10512–10516. [CrossRef]
90. Suhina, T.; Amirjalayer, S.; Woutersen, S.; Bonn, D.; Brouwer, A.M. Ultrafast dynamics and solvent-dependent deactivation kinetics of BODIPY molecular rotors. *Phys. Chem. Chem. Phys.* **2017**, *19*, 19998–20007. [CrossRef]
91. Thorat, K.G.; Ray, A.K.; Sekar, N. Modulating TICT to ICT characteristics of acid switchable red emitting boradiazaindacene chromophores: Perspectives from synthesis, photophysical, hyperpolarizability and TD-DFT studies. *Dyes Pigment.* **2017**, *136*, 321–334. [CrossRef]
92. Zhang, X.-F.; Feng, N. Photoinduced Electron Transfer-based Halogen-free Photosensitizers: Covalent meso-Aryl (Phenyl, Naphthyl, Anthryl, and Pyrenyl) as Electron Donors to Effectively Induce the Formation of the Excited Triplet State and Singlet Oxygen for BODIPY Compounds. *Chem. Asian J.* **2017**, *12*, 2447–2456. [CrossRef]
93. Leen, V.; Laine, M.; Ngongo, J.M.; Lipkowski, P.; Verbelen, B.; Kochel, A.; Dehaen, W.; van der Auweraer, M.; Nadtochenko, V.; Filarowski, A. Impact of the Keto-Enol Tautomeric Equilibrium on the BODIPY Chromophore. *J. Phys. Chem. A* **2018**, *122*, 5955–5961. [CrossRef]
94. Mallah, R.; Sreenath, M.C.; Chitrambalam, S.; Joe, I.H.; Sekar, N. Excitation energy transfer processes in BODIPY based donor-acceptor system—Synthesis, photophysics, NLO and DFT study. *Opt. Mater.* **2018**, *84*, 795–806. [CrossRef]
95. Ordóñez-Hernández, J.; Jiménez-Sánchez, A.; García-Ortega, H.; Sánchez-Puig, N.; Flores-Álamo, M.; Santillan, R.; Farfán, N. A series of dual-responsive Coumarin-Bodipy probes for local microviscosity monitoring. *Dyes Pigment.* **2018**, *157*, 305–313. [CrossRef]
96. Ripoll, C.; Cheng, C.; Garcia-Fernandez, E.; Li, J.; Orte, A.; Do, H.; Jiao, L.; Robinson, D.; Crovetto, L.; González-Vera, J.A.; et al. Synthesis and Spectroscopy of Benzylamine-Substituted BODIPYs for Bioimaging. *Eur. J. Org. Chem.* **2018**, *2018*, 2561–2571. [CrossRef]
97. Ali, H.; Guérin, B.; van Lier, J.E. gem-Dibromovinyl boron dipyrrins: Synthesis, spectral properties and crystal structures. *Dalton Trans.* **2019**, *48*, 11492–11507. [CrossRef] [PubMed]
98. Antina, L.A.; Ksenofontov, A.A.; Kalyagin, A.A.; Antina, E.V.; Berezin, M.B.; Khodov, I.A. Luminescent properties of new 2,2-, 2,3- and 3,3-CH2-bis(BODIPY)s dyes: Structural and solvation effects. *Spectrochim. Acta A Mol. Biomol. Spectrosc.* **2019**, *218*, 308–319. [CrossRef] [PubMed]
99. Bai, L.; Sun, P.; Liu, Y.; Zhang, H.; Hu, W.; Zhang, W.; Liu, Z.; Fan, Q.; Li, L.; Huang, W. Novel aza-BODIPY based small molecular NIR-II fluorophores for in vivo imaging. *Chem. Commun.* **2019**, *55*, 10920–10923. [CrossRef]
100. Guseva, G.B.; Ksenofontov, A.A.; Antina, E.V.; Berezin, M.B.; Vyugin, A.I. Effect of solvent nature on spectral properties of blue-emitting meso-propargylamino-BODIPY. *J. Mol. Liquids* **2019**, *285*, 194–203. [CrossRef]

101. Kawakami, J.; Sasaki, Y.; Yanase, K.; Ito, S. Benzo-fused BODIPY Derivative as a Fluorescent Chemosensor for Fe^{3+}, Cu^{2+}, and Al^{3+}. *Trans. Mat. Res. Soc. Jpn.* **2019**, *44*, 69–73. [CrossRef]
102. Sevinç, G.; Özgür, M.; Küçüköz, B.; Karatay, A.; Aslan, H.; Yılmaz, H. Synthesis and spectroscopic properties of a novel "turn off" fluorescent probe: Thienyl-pyridine substituted BODIPY. *J. Lumin.* **2019**, *211*, 334–340. [CrossRef]
103. Zhang, X.-F.; Zhu, J. BODIPY parent compound: Fluorescence, singlet oxygen formation and properties revealed by DFT calculations. *J. Lumin.* **2019**, *205*, 148–157. [CrossRef]
104. González-Vera, J.A.; Lv, F.; Escudero, D.; Orte, A.; Guo, X.; Hao, E.; Talavera-Rodriguez, E.M.; Jiao, L.; Boens, N.; Ruedas-Rama, M.J. Unusual spectroscopic and photophysical properties of solvatochromic BODIPY analogues of Prodan. *Dyes Pigment.* **2020**, *182*, 108510. [CrossRef]
105. Shen, F.; Wang, T.; Yu, X.; Li, Y. Free radical oxidation reaction for selectively solvatochromic sensors with dynamic sensing ability. *Chin. Chem. Lett.* **2020**, *31*, 1919–1922. [CrossRef]
106. Vyšniauskas, A.; Cornell, B.; Sherin, P.S.; Maleckaitė, K.; Kubánková, M.; Izquierdo, M.A.; Vu, T.T.; Volkova, Y.A.; Budynina, E.M.; Molteni, C.; et al. Cyclopropyl Substituents Transform the Viscosity-Sensitive BODIPY Molecular Rotor into a Temperature Sensor. *ACS Sens.* **2021**, *6*, 2158–2167. [CrossRef] [PubMed]
107. ChemAxon, JChem for Office. Available online: www.chemaxon.com (accessed on 7 April 2020).
108. López Arbeloa, T.; López Arbeloa, F.; López Arbeloa, I.; García-Moreno, I.; Costela, A.; Sastre, R.; Amat-Guerri, F. Correlations between photophysics and lasing properties of dipyrromethene–BF2 dyes in solution. *Chem. Phys. Lett.* **1999**, *299*, 315–321. [CrossRef]
109. Costela, A.; García-Moreno, I.; Gomez, C.; Sastre, R.; Amat-Guerri, F.; Liras, M.; López Arbeloa, F.; Bañuelos Prieto, J.; López Arbeloa, I. Photophysical and Lasing Properties of New Analogs of the Boron–Dipyrromethene Laser Dye PM567 in Liquid Solution. *J. Phys. Chem. A* **2002**, *106*, 7736–7742. [CrossRef]
110. Rohand, T.; Lycoops, J.; Smout, S.; Braeken, E.; Sliwa, M.; van der Auweraer, M.; Dehaen, W.; Borggraeve, W.M.D.; Boens, N. Photophysics of 3,5-diphenoxy substituted BODIPY dyes in solution. *Photochem. Photobiol. Sci.* **2007**, *6*, 1061–1066. [CrossRef]
111. Costela, A.; García-Moreno, I.; Pintado-Sierra, M.; Amat-Guerri, F.; Liras, M.; Sastre, R.; Arbeloa, F.L.; Bañuelos Prieto, J.; Arbeloa, I.L. New laser dye based on the 3-styryl analog of the BODIPY dye PM567. *J. Photochem. Photobiol. A Chem.* **2008**, *198*, 192–199. [CrossRef]
112. Arroyo, I.J.; Hu, R.; Merino, G.; Tang, B.Z.; Peña-Cabrera, E. The smallest and one of the brightest. Efficient preparation and optical description of the parent borondipyrromethene system. *J. Org. Chem.* **2009**, *74*, 5719–5722. [CrossRef]
113. Costela, A.; García-Moreno, I.; Pintado-Sierra, M.; Amat-Guerri, F.; Sastre, R.; Liras, M.; López Arbeloa, F.; Bañuelos Prieto, J.; López Arbeloa, I. New analogues of the BODIPY dye PM597: Photophysical and lasing properties in liquid solutions and in solid polymeric matrices. *J. Phys. Chem. A* **2009**, *113*, 8118–8124. [CrossRef]
114. Bañuelos, J.; Arroyo-Córdoba, I.J.; Valois-Escamilla, I.; Alvarez-Hernández, A.; Peña-Cabrera, E.; Hu, R.; Zhong Tang, B.; Esnal, I.; Martínez, V.; López Arbeloa, I. Modulation of the photophysical properties of BODIPY dyes by substitution at their meso position. *RSC Adv.* **2011**, *1*, 677. [CrossRef]
115. Bañuelos, J.; Martín, V.; Gómez-Durán, C.F.A.; Arroyo Córdoba, I.J.; Peña-Cabrera, E.; García-Moreno, I.; Costela, Á.; Pérez-Ojeda, M.E.; Arbeloa, T.; López Arbeloa, I. New 8-amino-BODIPY derivatives: Surpassing laser dyes at blue-edge wavelengths. *Chem. A Eur. J.* **2011**, *17*, 7261–7270. [CrossRef]
116. Duran-Sampedro, G.; Agarrabeitia, A.R.; Garcia-Moreno, I.; Costela, A.; Bañuelos, J.; Arbeloa, T.; López Arbeloa, I.; Chiara, J.L.; Ortiz, M.J. Chlorinated BODIPYs: Surprisingly Efficient and Highly Photostable Laser Dyes. *Eur. J. Org. Chem.* **2012**, *2012*, 6335–6350. [CrossRef]
117. Osorio-Martínez, C.A.; Urías-Benavides, A.; Gómez-Durán, C.F.A.; Bañuelos, J.; Esnal, I.; López Arbeloa, I.; Peña-Cabrera, E. 8-AminoBODIPYs: Cyanines or hemicyanines? The effect of the coplanarity of the amino group on their optical properties. *J. Org. Chem.* **2012**, *77*, 5434–5438. [CrossRef]
118. Zhang, M.; Hao, E.; Xu, Y.; Zhang, S.; Zhu, H.; Wang, Q.; Yu, C.; Jiao, L. One-pot efficient synthesis of pyrrolylBODIPY dyes from pyrrole and acyl chloride. *RSC Adv.* **2012**, *2*, 11215. [CrossRef]
119. Durán-Sampedro, G.; Agarrabeitia, A.R.; Cerdán, L.; Pérez-Ojeda, M.E.; Costela, A.; García-Moreno, I.; Esnal, I.; Bañuelos, J.; Arbeloa, I.L.; Ortiz, M.J. Carboxylates versus Fluorines: Boosting the Emission Properties of Commercial BODIPYs in Liquid and Solid Media. *Adv. Funct. Mater.* **2013**, *23*, 4195–4205. [CrossRef]
120. Esnal, I.; Urías-Benavides, A.; Gómez-Durán, C.F.A.; Osorio-Martínez, C.A.; García-Moreno, I.; Costela, A.; Bañuelos, J.; Epelde, N.; López Arbeloa, I.; Hu, R.; et al. Reaction of amines with 8-methylthioBODIPY: Dramatic optical and laser response to amine substitution. *Chem. Asian J.* **2013**, *8*, 2691–2700. [CrossRef] [PubMed]
121. Esnal, I.; Valois-Escamilla, I.; Gómez-Durán, C.F.A.; Urías-Benavides, A.; Betancourt-Mendiola, M.L.; López-Arbeloa, I.; Bañuelos, J.; García-Moreno, I.; Costela, A.; Peña-Cabrera, E. Blue-to-orange color-tunable laser emission from tailored boron-dipyrromethene dyes. *Chemphyschem* **2013**, *14*, 4134–4142. [CrossRef] [PubMed]
122. Flores-Rizo, J.O.; Esnal, I.; Osorio-Martínez, C.A.; Gómez-Durán, C.F.A.; Bañuelos, J.; López Arbeloa, I.; Pannell, K.H.; Metta-Magaña, A.J.; Peña-Cabrera, E. 8-Alkoxy- and 8-aryloxy-BODIPYs: Straightforward fluorescent tagging of alcohols and phenols. *J. Org. Chem.* **2013**, *78*, 5867–5877. [CrossRef]
123. Choi, S.; Bouffard, J.; Kim, Y. Aggregation-induced emission enhancement of a meso-trifluoromethyl BODIPY via J-aggregation. *Chem. Sci.* **2014**, *5*, 751–755. [CrossRef]

124. Liu, C.-L.; Chen, Y.; Shelar, D.P.; Li, C.; Cheng, G.; Fu, W.-F. Bodipy dyes bearing oligo(ethylene glycol) groups on the meso-phenyl ring: Tuneable solid-state photoluminescence and highly efficient OLEDs. *J. Mater. Chem. C* **2014**, *2*, 5471. [CrossRef]
125. Filatov, M.A.; Karuthedath, S.; Polestshuk, P.M.; Callaghan, S.; Flanagan, K.J.; Telitchko, M.; Wiesner, T.; Laquai, F.; Senge, M.O. Control of triplet state generation in heavy atom-free BODIPY-anthracene dyads by media polarity and structural factors. *Phys. Chem. Chem. Phys.* **2018**, *20*, 8016–8031. [CrossRef]
126. Prasannan, D.; Arunkumar, C. A "turn-on-and-off" pH sensitive BODIPY fluorescent probe for imaging E. coli cells. *N. J. Chem.* **2018**, *42*, 3473–3482. [CrossRef]
127. Zhang, X.-F.; Feng, N. Attaching naphthalene derivatives onto BODIPY for generating excited triplet state and singlet oxygen: Tuning PET-based photosensitizer by electron donors. *Spectrochim. Acta A Mol. Biomol. Spectrosc.* **2018**, *189*, 13–21. [CrossRef] [PubMed]
128. Belmonte-Vázquez, J.L.; Avellanal-Zaballa, E.; Enríquez-Palacios, E.; Cerdán, L.; Esnal, I.; Bañuelos, J.; Villegas-Gómez, C.; López Arbeloa, I.; Peña-Cabrera, E. Synthetic Approach to Readily Accessible Benzofuran-Fused Borondipyrromethenes as Red-Emitting Laser Dyes. *J. Org. Chem.* **2019**, *84*, 2523–2541. [CrossRef] [PubMed]
129. Hu, W.; Lin, Y.; Zhang, X.-F.; Feng, M.; Zhao, S.; Zhang, J. Heavy-atom-free charge transfer photosensitizers: Tuning the efficiency of BODIPY in singlet oxygen generation via intramolecular electron donor-acceptor interaction. *Dyes Pigment.* **2019**, *164*, 139–147. [CrossRef]
130. Hu, W.; Liu, M.; Zhang, X.-F.; Wang, Y.; Wang, Y.; Lan, H.; Zhao, H. Can BODIPY-Electron Acceptor Conjugates Act as Heavy Atom-Free Excited Triplet State and Singlet Oxygen Photosensitizers via Photoinduced Charge Separation-Charge Recombination Mechanism? *J. Phys. Chem. C* **2019**, *123*, 15944–15955. [CrossRef]
131. Mallah, R.R.; Mohbiya, D.R.; Sreenath, M.C.; Chitrambalam, S.; Joe, I.H.; Sekar, N. NLOphoric benzyl substituted BODIPY and BOPHY: A comprehensive linear and nonlinear optical study by spectroscopic, DFT and Z-scan measurement. *Spectrochim. Acta A Mol. Biomol. Spectrosc.* **2019**, *215*, 122–129. [CrossRef] [PubMed]
132. Mallah, R.R.; Mohbiya, D.R.; Sreenath, M.C.; Chitrambalam, S.; Joe, I.H.; Sekar, N. Non-linear optical response of meso hybrid BODIPY: Synthesis, photophysical, DFT and Z scan study. *Spectrochim. Acta A Mol. Biomol. Spectrosc.* **2019**, *209*, 126–140. [CrossRef]
133. Zhang, X.-F.; Zhu, J. BODIPY parent compound: Excited triplet state and singlet oxygen formation exhibit strong molecular oxygen enhancing effect. *J. Lumin.* **2019**, *212*, 286–292. [CrossRef]
134. Berezin, M.B.; Antina, E.V.; Guseva, G.B.; Kritskaya, A.; Semeikin, A.S. Effect of meso-phenyl substitution on spectral properties, photo- and thermal stability of boron (III) and zinc (II) dipyrrometenates. *Inorg. Chem. Commun.* **2020**, *111*, 107611. [CrossRef]
135. DataWarrior: An Open-Source Program for Data Visualization and Analysis with Chemical Intelligence. Available online: https://openmolecules.org/datawarrior/ (accessed on 2 November 2021).
136. Backman, T.W.; Cao, Y.; Girke, T. ChemMine Tools: An Online Service for Analyzing and Clustering Small Molecules. Available online: https://chemminetools.ucr.edu/ (accessed on 2 November 2021).
137. Liptay, W. Die Lösungsmittelabhängigkeit der Wellenzahl von Elektronenbanden und die chemisch-physikalischen Grundlagen. *J. Phys. Sci. Z. Naturforschung A* **1965**, *20*, 1441–1471. [CrossRef]
138. SCImago Graphica Beta 1.0.12. Available online: www.graphica.app (accessed on 2 November 2021).
139. Kawski, A.; Kukliński, B.; Bojarski, P.; Diehl, H. Ground and Excited State Dipole Moments of LAURDAN Determined from Solvatochromic and Thermochromic Shifts of Absorption and Fluorescence Spectra. *Z. Für Nat.* **2000**, *55a*, 817–822. [CrossRef]
140. Kawski, A. On the Estimation of Excited-State Dipole Moments from Solvatochromic Shifts of Absorption and Fluorescence Spectra. *Z. Für Nat.* **2002**, *57a*, 255–262. [CrossRef]
141. Minkin, V.I.; Osipov, O.A.; Zhdanov, I.A. *Dipole Moments in Organic Chemistry*; Plenum Press: New York, NY, USA, 1970.
142. Reichardt, C.; Welton, T. *Solvents and Solvent Effects in Organic Chemistry*, 4th ed.; Wiley-VCH: Weinheim, Germany, 2011; ISBN 3527324739.
143. Lakowicz, J.R. *Principles of Fluorescence Spectroscopy*, 3rd ed.; Springer: New York, NY, USA, 2006; ISBN 0387312781.
144. Bakhshiev, N.G.; Knyazhanskii, M.I.; Minkin, V.I.; Osipov, O.A.; Saidov, G.V. Experimental Determination of the Dipole Moments of Organic Molecules in Excited Electronic Statesf. *Russ. Chem. Rev.* **1969**, *38*, 740–754. [CrossRef]
145. Liptay, W. Dipole Moments and Polarizabílítíes of Molecules in Excited Electronic States. *Excit. States* **1974**, *1*, 129–229.
146. Marsh, D. Reaction Fields in the Environment of Fluorescent Probes: Polarity Profiles in Membranes. *Biophys. J.* **2009**, *96*, 2549–2558. [CrossRef]
147. Randles, E.G.; Bergethon, P.R. Reaction Field Analysis and Lipid Bilayer Location for Lipophilic Fluorophores. *J. Phys. Chem. B* **2013**, *117*, 10193–10202. [CrossRef]
148. Cerón-Carrasco, J.P.; Jacquemin, D.; Laurence, C.; Planchat, A.; Reichardt, C.; Sraïdi, K. Solvent polarity scales: Determination of new ET (30) values for 84 organic solvents. *J. Phys. Org. Chem.* **2014**, *27*, 512–518. [CrossRef]
149. Varhese, A.; Akshaya, K.B. Application of Fluorescence in Solvatochromic Studies of Organic Compounds. In *Reviews in Fluorescence 2017*; Geddes, C.D., Ed.; Springer International Publishing: Cham, Switzerland, 2018; pp. 99–121, ISBN 978-3-030-01568-8.